

**VOLATILES CHARACTERIZATION DURING WHISKEY PRODUCTION
USING HEADSPACE – SOLID PHASE MICROEXTRACTION – GAS
CHROMATOGRAPHY – MASS SPECTROMETRY**

by

ROBERT H. MAGNUSON II

THESIS

Submitted in partial fulfillment of the requirements for the degree of

Master of Science in Chemistry

at The University of Texas at Arlington

December 2021

Arlington, Texas

Supervising Committee:

Kevin A. Schug, Supervising Professor

Purnendu Dasgupta

Kayunta Johnson-Winters

Acknowledgements

First, I want to express my gratitude to Dr. Kevin A. Schug, whose mentorship, assistance, and patience has been invaluable during my time here and without whom, I wouldn't be here today.

Secondly, I would like to thank my committee members, Dr. Purnendu Dasgupta and Dr. Kayunta Johnson-Winters, for their time and assistance, with special consideration to Dr. Dasgupta for allowing me extensive access to his lab during all of my troubleshooting endeavors.

Thirdly, I want to thank all of the group members of the Schug lab who have helped me immeasurably throughout my years here. This list includes, but is not limited to, Dr. Tiffany Liden, Dr. Paige Wicker, Dr. Hailee Ratcliffe, Dr. Emmanuel Varona-Torres, Dr. Jamie York, Dr. Jonathan Thacker, Dr. Blair Berger, Dino Camdzic, Michelle Camdzic, Michael Pecore, Josh Isaacs, Shannon Thomas, Brady Drennan, and Emily Preuss. You have all been a font of knowledge and inspiration that has made my experience here all the more beneficial.

I would like to give a special mention to Dr. Philip Shelor, of Dr. Dasgupta's lab, whose expansive expertise and unwavering patience helped me on innumerable occasions.

Finally, I would like to thank my family for their understanding, patience, and above all, faith in me. Their belief in me never wavered, even when I felt I didn't belong.

Table of Contents

Acknowledgements	1
List of Abbreviations	3
List of Tables	4
List of Figures	5
Abstract	6
Background	7
Method	9
Results and Discussion	11
Conclusion	20
References	21
Supplemental Information	26

List of Abbreviations

HS: Headspace

SPME: Solid phase microextraction

GC/MS: Gas chromatography / Mass spectrometry

In-Ex: Incubation and Extraction

R: Red corn sample

W: White corn sample

Y: Yellow corn sample

B: Indigo Blue corn sample

G: Waxy Yellow Dent corn sample

bu: bushel

EtOH: ethanol

NaCl: sodium chloride

IL-1: 1-Ethyl-3-methylimidazolium ethyl sulfate

IL-2: 1-Ethyl-3-methylimidazolium bis(trifluoromethanesulfonyl) imide

USD: United States dollar

NIST: National Institute of Standards and Technology

CRM: Certified reference material

List of Tables

Table S1. Compound ID's, ordered for PLS-DA heat map, for Dry Corn HS/SPME sampling PCA and PLS-DA treatments.	27
Table S2. VIP Compounds for Waxy Dent (G) dry maize	30
Table S3. VIP Compounds for Yellow (Y) dry maize	30
Table S4. VIP Compounds for Blue (B) dry maize	31
Table S5. VIP Compounds for Red (R) dry maize	31
Table S6. VIP Compound for White (W) dry maize	31
Table S7. Compound ID's for liquid mash sampling	36
Table S8. Compound ID's for HS/SPME injection of Red (R) mash	40
Table S9. Compound ID's for HS/SPME injection of White (W) mash	40
Table S10. Compound ID's for HS/SPME injection of Yellow (Y) mash	40
Table S11. Compound ID's for HS/SPME injection of Blue (B) mash	41
Table S12. Compound ID's for HS/SPME injection of Waxy Dent (G) mash	41
Table S13. Compound ID's for HS/SPME injection of Red (R) beer	43
Table S14. Compound ID's for HS/SPME injection of White (W) beer	43
Table S15. Compound ID's for HS/SPME injection of Yellow (Y) beer	43
Table S16. Compound ID's for HS/SPME injection of Blue (B) beer	44

List of Figures

Figure 1. Typical whiskey production scheme	7
Figure 2. Chromatograms of HS/SPME injection dry maize samples	13
Figure 3. PCA scores plot from HS/SPME injection of dry maize	14
Figure 4. Top 15 VIP compounds from PLS-DA for HS/SPME dry maize samples	15
Figure 5. Condensed PLS-DA generated heat map	16
Figure 6. Chromatograms of liquid mash injections	17
Figure 7. Chromatograms of liquid injection of beer samples	18
Figure 8. Chromatograms of HS/SPME injection of mash samples	18
Figure 9. Chromatograms of HS/SPME injection of beer samples	19
Figure S1. HS/SPME of dry maize samples, enlarged	26
Figure S2. Enlarged PLS-DA heat map for HS/SPME of dry maize samples	32
Figure S3. Chromatograms of liquid injection of mash samples, enlarged	35
Figure S4. Chromatograms of liquid injection of beer samples, enlarged	38
Figure S5. Chromatograms for HS/SPME injection of mash samples, enlarged	39
Figure S6. Chromatograms for HS/SPME injection beer samples, enlarged	42

Abstract

Whiskey is the second most consumed distilled alcoholic beverage type, by brand, on the planet behind Chinese Baijiu. A prominent component in many varieties of whiskey, maize, contributes a wide profile of compounds that undergo modification in the production pathway, ultimately influencing the final flavor profile. In this study, headspace/solid phase microextraction-gas chromatography/mass spectrometry (HS/SPME-GC/MS) was used to characterize the volatile profile of 5 different maize varieties, mashes produced from each, and 4 post-fermentation mixtures. Headspace sampling was performed using a high capacity SPME Arrow device, in an effort maximize the species detected. Compound identification was supplied by matches within the NIST17 library of compound spectra. The statistical treatments of principal component analysis (PCA) and partial least squares discriminant analysis (PLS-DA) were used on a 143-peak list derived from the dried maize samplings as an effort to substantiate visual, qualitative differences between the 5 varieties' volatile profiles. Mash and beer samples prepared from 4 of the maize cultivars were compared with both liquid injections and HS/SPME analyses, with greater differences apparent amongst the beers, in either introduction method. The species observed across the analyses are consistent with glycolytic and fermentation products, suggesting that the HS/SPME sampling parameters on the dried maize served as a pseudo- "dry mashing" procedure.

Background

Global consumption of alcohol in 2019 has been estimated at 6.4 L per capita of pure ethanol (EtOH), with 1.66 L per capita attributed to the consumption of distilled spirits.¹ This showed an increase of approximately of 0.61% in spirits consumption over the previous year, accounting for approximately 820,000 L of increased consumption.^{1,2} Of the total spirits consumed, the estimates on whiskey consumption in 2019 approach 6.46 billion L³. This amounts to an estimated 61.75 billion USD in 2019 market value and is projected to reach almost 100 billion USD by 2026⁴. The popularity of whiskey has likewise increased, where the number of whiskey distilleries in the U.S. increased from 90 in 2011 to 657 in 2021⁵.

To name a beverage “Whiskey” in the US, it must be a distillate of fermented grain at less than 95% EtOH (% v/v) content, stored in oak containers, packaged at 40% EtOH (% v/v) content or higher, and generally seem like a whiskey⁶. While additional restrictions are outlined as requirements for certain sub-classes (e.g. bourbon), the parent definition is quite permissive and even includes mixtures described as “otherwise undefined”⁶. These expansive permissions have fostered a market of myriad expressions, from a Shakespeare-inspired Christmas whiskey meant to invoke the warmth of a cold winters’ night, to a Thai Snake whiskey which sells with a poisonous cobra in the bottle and asserts a heat distinct from any good intentions^{7,8}.

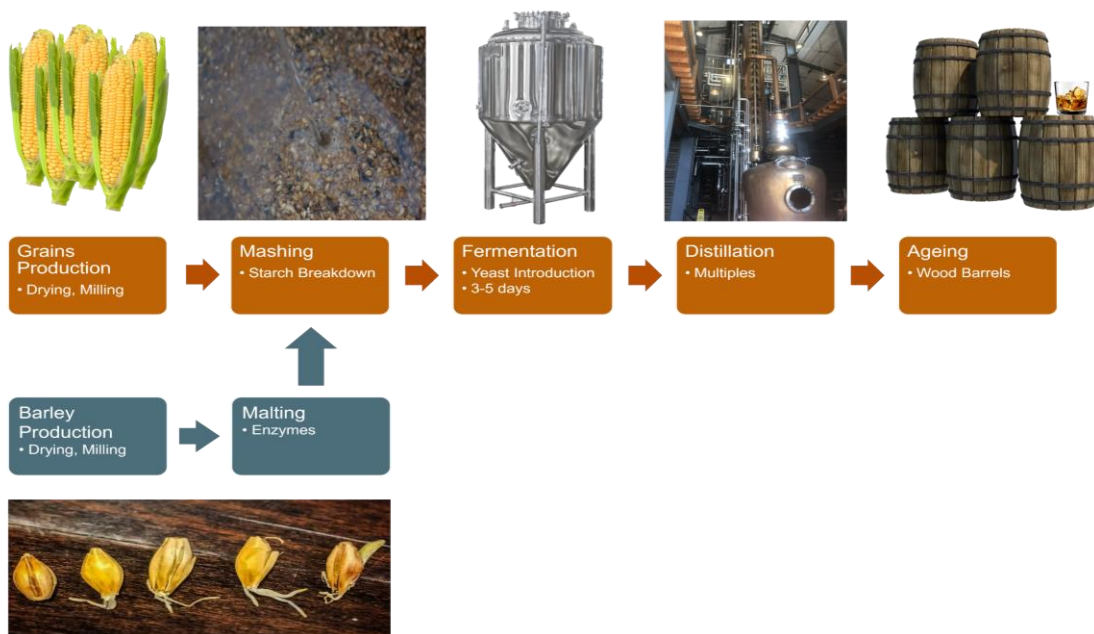


Figure 1. Typical whiskey production scheme

Whiskey production (Fig. 1) has five basic steps: 1) choosing the type and ratio of the grains used, or the “mash bill”; 2), “mashing” the grains by heating in a water bath; 3),

adding yeast to the mash for fermentation; 4), distilling the beer; and finally, 5) aging the distillate, or “new make,” in a barrel.

The common choices for grains used are maize (corn), wheat, and barley; although, other grains can be selected and incorporated for stylistic desires or for novelty⁸⁻¹⁰. In the US., maize is the most common grain used, and is actually required to be the majority grain component in bourbon⁶. Maize also dominates mash bills in eastern Canada, and some grain whiskies used for the production of blended whiskies in Scotland, Ireland, and Japan, but is scarce in Indian whiskies¹¹⁻¹⁸.

In 2019, US. maize production was estimated at 13.6 billion bushels overall, with the use attributed to alcoholic beverage production at 41.1 million bushels, a 16% increase over the year prior. Beverage use in 2020 showed a small increase to 42.4 million bushels out of 14.1 billion bushels produced overall. Projected corn production in 2021/2022 in the U.S. is expected to be approximately 15.1 billion bushels, with a currently estimated usage thus far at 30.4 million bushels for the production of alcoholic beverages¹⁹⁻²³. The production scale of maize in the US., and owing to its main uses being livestock feed or ethanol production^{19,20}, has prioritized a cultivar that prioritizes yield and efficiency²⁴. However, the resulting decrease in the genetic diversity of grains produced might be limiting the flavor expressions that are available to separate, more unique strains²⁵.

Maize is harvested and given its valuation, or graded, based on a number of factors, but one of the most critical is the moisture content^{26,27}. A bushel of maize weighs 56 lbs. (25.40 kg), by definition; however, the amount of usable dry grain varies with the moisture content, reported as water % (w/w). In order to maximize both the producer's revenue and to prevent microbial and fungal spoilage, the maize is further dried after harvesting, typically to 15% (w/w) at most. There are a number of common drying methods²⁸⁻³², the most frequent of these being the grain silo where heated air, typically 37.8-65.6 °C, is pumped upwards through the drying grain; a process that can take multiple weeks, or even months³¹.

Once dried, the maize can be milled, if desired, and is then cooked with water and malted barley, or malt extract, to solubilize the starches and break them down to the simpler sugars required for the subsequent yeast fermentation. Once the yeast is pitched, fermentation typically lasts 3-5 days, where it can then be transferred to the still¹¹. Distillation yields a final product that is then processed according the desired final style, such as charcoal filtering for a typical Tennessee whiskey, before it is aged in a wood barrel.

Volatiles analysis using HS/SPME has primarily focused on wines³³⁻³⁵, though whiskey and precursor grains have shown to be of some interest, as well³⁶⁻⁴². A powerful motivator in addition to health and safety monitoring is the identification of falsified

vintages^{43,44}, which are typically prepared from a cheaper whiskey or grain alcohol and then intentionally dosed with compounds (e.g. 3-methylbutanol⁴⁵) associated with older, traditionally-aged spirits. An infamous investigation⁴⁶ into assessing the efficacy of the classically trained and experienced sensory experts showed that they were able to easily differentiate between an authentic blended scotch and a synthetic analogue; however, less than 10% were successful if the synthetic beverage was mixed in equal portions with the authentic one. With the export market for scotch whiskey estimated at over 5 billion USD⁴⁷, the continual search for powerful analytical modalities to identify these counterfeits is ever evolving.

The primary aim of this study was to identify major species within the precursor maize, mash, and beer samples, and to potentially observe their transformation throughout the production process using the pre-concentrative power of the solid phase microextraction (SPME) modality combined with the long-established elucidatory capabilities of a mass spectrometer coupled to a gas chromatograph. Principal component analysis (PCA) and partial least squares discriminant analysis (PLS-DA) were incorporated into the design in order to supplement qualitative determinations on the dry maize differentiations.

Method

Chemicals and Supplies

Mass spectrometry (MS) grade water (Honeywell, Charlotte, NC, USA), MS grade methanol (J.T.Baker, Phillipsburg, NJ, USA) and sodium chloride (NaCl, ≥99 %, Fisher Chemical, Fair Lawn, NJ, USA) were sourced from VWR (VWR International, Radnor, PA, USA). 1-Ethyl-3-methylimidazolium ethyl sulfate (IL-1) and 1-ethyl-3-methylimidazolium bis(trifluoromethanesulfonyl) imide (IL-2) were sourced from Sigma-Aldrich (Sigma-Aldrich Inc., St. Louis, MO, USA). 10-mL HS Vials sealed by screw caps equipped with 1.5 mm PTFE/Silicone septa and 20-mL HS vials sealed by crimp top bimetallic caps equipped with PTFE/Silicone septa were sourced from Restek (Restek Corporation, Bellefonte, PA, USA).

Dry Corn Preparation

Five non-GMO organic corns; Indigo Blue (B); Red (R); White (W); Yellow (Y); and Waxy Dent (G) were sourced from Clarkson (Clarkson Grain Company, Cerro Gordo, IL, USA). As described by Clarkson, the grains were dried in a bottom-flow vent dryer to attain a moisture content of 14.5% using air heated to approximately 105-110 °F (40.6-43.3 °C)⁴⁸. The dried maize was cryogenically milled in 20 g aliquots using a Retsch Cryomill (Haan, NRW, GmbH) at 3 cycles of 30 Hz frequency, with 1 minute of pre-cooling and post-cooling between each repetition. All milled samples were stored at -10 °C afterwards for subsequent analysis.

Instrumentation

A Shimadzu 2010-Plus gas chromatograph coupled with TQ-8030 mass spectrometer (Shimadzu Scientific Instruments, Columbia, MD, USA) and equipped with an AOC-6000 autosampler was used for analysis. Analyses were performed using a Restek RXI-5SilMS (30 m x 0.25 mm ID x 0.25 μm df) capillary column with helium as a carrier gas. The MS was operated in Q3 scan mode, with the acquisition range set to 55-500 m/z. For analytical HS/SPME samplings, a di-phasic divinylbenzene/polydimethylsiloxane (DVB/PDMS) SPME Arrow fiber (Restek Corporation, Bellefonte, PA, USA) was used, with a phase thickness and length of 120 μm and 20 mm, respectively. Pre- and post-conditioning of the SPME fiber were conducted for 5 minutes at 250 $^{\circ}\text{C}$, with a gas flow of 1.2 mL min^{-1} and a split ratio of 30:1. Additionally, an initial conditioning for 30 minutes prior to each batch analysis was performed. During the initial parameter screening, the aforementioned di-phasic fiber was screened against a tri-phasic divinylbenzene/polydimethylsiloxane/carbon wide range (DVB/PDMS/CWr) SPME Arrow fiber (Restek Corporation), again with a phase thickness and length of 120 μm and 20 mm, respectively. For liquid samplings, a Hamilton 10- μL syringe (Hamilton, Reno, NV, USA) was utilized and was pre- and post-rinsed 3 times with a 50% aqueous methanol mixture in between each run.

Analysis of Dried Corn

Sample parameter screening and optimization was performed with respect to sample amount, paired extraction and incubation temperatures, individual incubation and extraction times, and presence of a liquid additive in the 20-mL HS vials that were used. These screenings are outlined further in Supplemental Tables 1-3. Water used was MS grade. IL-1 and IL-2 were cleaned with stirred heating at 90 $^{\circ}\text{C}$ under a nitrogen stream for 24 hours prior to use. For the analytical runs, 2.50 g of each sample type was placed in 20-mL HS vials. Vials were sampled with incubation and extraction periods of 40 minutes and 20 minutes, respectively, thermostated at 120 $^{\circ}\text{C}$. Samples were desorbed for 2 minutes at 230 $^{\circ}\text{C}$ in splitless mode, whereafter a split ratio of 5:1 was implemented. The chromatograph was operated in constant velocity mode at 45.1 cm sec^{-1} , with a column flow of 1.56 mL min^{-1} . Temperature programming began at 40 $^{\circ}\text{C}$ with a 2-minute initial hold, was raised to 100 $^{\circ}\text{C}$ at 5 $^{\circ}\text{C min}^{-1}$ and held for 1 minute, and finally raised to 255 $^{\circ}\text{C}$ at 4 $^{\circ}\text{C min}^{-1}$ with a final hold time of 10 minutes, giving a total run time of 64 minutes. Analyses were performed in quadruplicate.

Analysis of Mash and Beer

For four varieties (R, W, B, and Y), limited sample size compelled an initially conservative use of the beer and mash samples. They were first analyzed using 1- μL liquid injections in split mode, with a split ratio of 5:1. The chromatograph was operated in constant velocity mode at 45.1 cm sec^{-1} , with a column flow of 1.56 mL min^{-1} .

Temperature programming began at 40 °C with a 1-minute initial hold, then raised to 200 °C at 10 °C min⁻¹ and held for 20 seconds, then finally raised to 320 °C at 20 °C min⁻¹ and held for 15 minutes, giving a total analysis time of 29 minutes. Analyses were performed in tetraplicate.

Additional runs were performed using HS/SPME samplings, again on R, W, B, and Y, though only singularly. Briefly, 500 µL of liquid beer or mash was diluted with 1.5 mL of MS grade water into a 10-mL HS vial. Samples were incubated and extracted at 50 °C, for 20 minutes and 30 minutes, respectively. The temperature programming and flow settings were as described for the liquid injections.

Waxy Dent (G) mash samples were prepared by centrifuging 4 separate 15 mL aliquots at 1800 G for 10 min to remove the suspended grain particulates, with the supernatant removed and combined for subsequent analysis. Into a 20-mL HS vial was added to 6 g of NaCl, followed 1 mL of the mash supernatant that was then diluted with 4 mL of water.

Retention Indices

Retention index values (RI) were developed⁴⁹ for each of the aforementioned analysis procedures by performing 1 µL liquid injections of a C₇-C₄₀ alkane CRM (Sigma-Aldrich, St. Louis, MO, USA) diluted to 100 µg mL⁻¹ each with MS grade n-hexane (Merck, Darmstadt, Hesse, GmbH). Index analyses were performed in quintuplicate.

Statistical Treatments

Secondary statistical treatments were performed using MetaboAnalyst 5.0⁵⁰ after peak processing for integration and compound identification, using the NIST17.1, NIST17.2, and NIST17s library volumes, within the GCMSolutions software (Shimadzu Scientific Instruments, Columbia, MD). Determined compound ID's correspond to an 80% similarity index match or greater, unless otherwise noted.

Results and Discussion

The first item screened was the stationary phase on the SPME Arrow. Of the two screened, use of the DVB/PDMS bi-phasic fiber gave consistently higher abundances over the tri-phasic fiber using 2.0 g of dried maize. All subsequent screenings proceeded using the DVB/PDMS fiber.

Table 1. Initial screening parameters for incubation and extraction temp. and time. (Total = 60 min, n=2)

Temperature (°C)	Incubation Time (min.)		
	20	30	40
60	2.0 g		
70			
80			
90	1.0, 2.0, & 3.0 g		
100			
110			
120			
130			
140			

The initial parameter screening (Table 1.) showed little results for any of the maize samples tested at an incubation/extraction (In-Ex) temperature below 80 °C, including analyses incorporating the presence of a liquid additive. Where signal peaks were apparent, they were barely differentiable from baseline noise, and attempts at identification were impeded by insufficient mass peak signals. This is consistent with standard, high-volume air drying techniques used such that the temperatures, air volume, and duration frequently employed would serve to volatilize the lower-boiling components that would have been present prior to the drying process^{28,30,31}.

Table 2. H₂O additive Screening (50 °C, 60 °C, 70 °C, 80 °C, n=2) (*: 50 °C & 80 °C only)

Mass (g)	Vol. (mL)	Vol. (mL)	Vol. (mL)	Vol. (mL)	Vol. (mL)
0.5*	0.300	0.500	1.000	1.500	2.000
1.0	0.500	1.000	1.500	2.000	2.500
1.5*	1.000	1.500	2.000	3.000	
2.0	1.500	2.000	3.000	4.000	
2.5*	2.000	3.000	4.000	5.000	
3.0	2.500	3.000	4.000	5.000	

The samples screened with H₂O (Table 2) showed an additional complication at In-Ex temperatures above 50 °C in that a gelatinous emulsion formed during the 1-hour period. This emulsion did not rectify once cooled to room temperature, and increased the occupied volume of the HS vial, precluding analysis. Emulsion formation was not seen with the ionic liquids screened, IL-1 and IL-2 (Table 3).

Table 3. IL-1 and IL-2 additive screening (80 °C & 100 °C, n=2)

Mass (g)	Vol. (mL)	Vol. (mL)	Vol. (mL)
0.5	0.500	1.000	1.500
1.0	1.000	1.500	2.000
2.0	2.000		4.000
3.0	3.000	4.000	

Their use allowed for an increase in In-Ex temperatures up to 110 °C and were selected for their hydrophilicity and hydrophobicity, respectively. Increases in signals were seen with the use of IL-2 relative to IL-1; however, the signals were diminished in both quantity and intensity compared to runs of the solo dried maize above 110 °C. For the sample amount screening, little difference was seen with amounts above 2.5 g, suggesting that the HS was saturated, making this the choice for analytical runs.

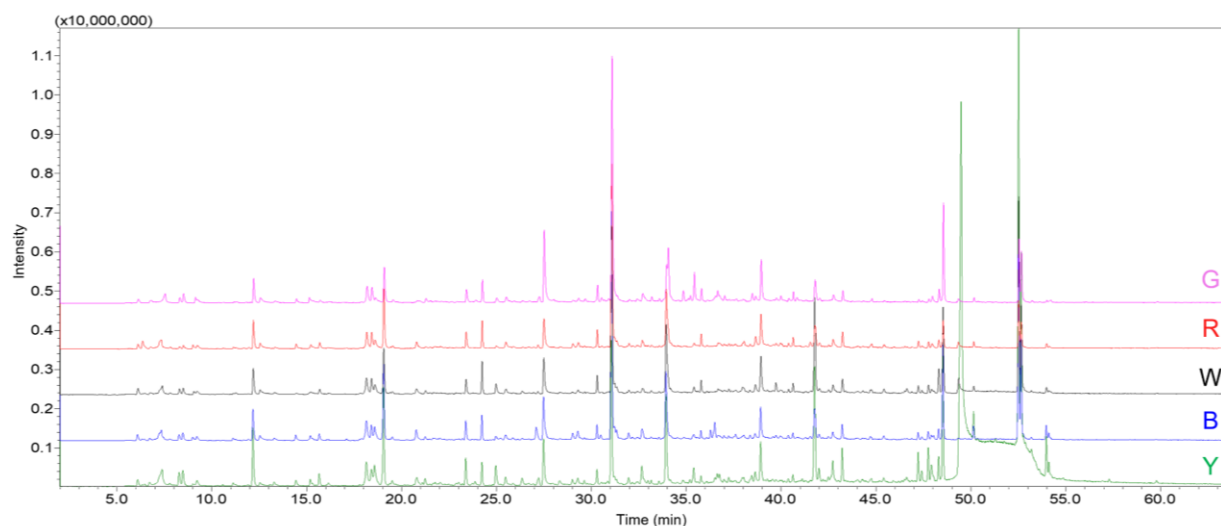


Figure 2. Chromatograms of HS/SPME injection of Waxy Dent (G), Red (R), White (W), Yellow (Y), and Blue (B) dry maize samples. Enlarged version is given as supplementary Figure S1.

The HS/SPME results on the dry maize (Fig. 2) indicate marked similarities for the samples at the lower temperatures (retention time (t_R) < 35.0 min), with differences arising in the form of increased signals for the Y samples thereafter. Of note, the Y samples showed a considerable concentration of hexadecanoic acid (Fig. S1, ID#130), its ethyl ester (Fig. S1, ID#131), the methyl ester of 9-octadecynoic acid (Fig. S1, ID#134), and linoleyl acetate (Fig. S1, ID#139). These ID's are consistent with other findings^{36-38,45}, including compounds previously reported in finished whiskey⁵¹.

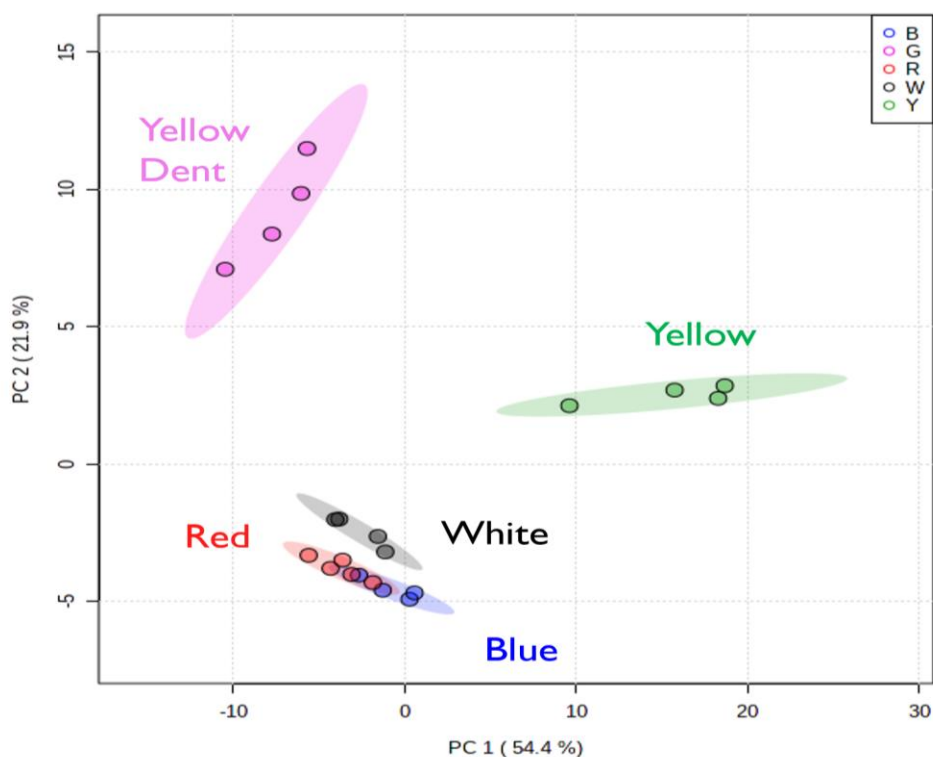


Figure 3. PCA scores plot generated from peak tables associated with HS/SPME injection of Yellow (green), Yellow Waxy Dent (pink), Blue (blue), Red (red), and White (black) dry maize samplings.

Scores generated from the PCA treatment (Fig. 3) were produced from a peak table of the compiled peak area integrations for 143 compounds selected based on repeatability in retention time (tR) and abundance. The plot indicates a high degree of differentiation for the G and Y samples from the other 3 maize varieties based on the peak table used (Table S4), with poor separation of the W set from R and B, but still appreciably separated from the G and Y sets. The R and B samples exhibit a high degree of overlap, indicating that the peaks chosen for the unguided analyses were insufficient to distinguish between these varieties. The R and B sets can be visually distinguished based on their respective chromatograms; however, the high intensity of their shared peak ID's appear to overshadow the differences that are seen in the less abundant species. It is worth noting that, in consideration of only principal component 1 (PC1) and principal component 2 (PC2), the model produced a 76.3% differentiating power. This number increases to 85.6% with the inclusion of the determined third principal component (PC3). This is suggestive that, while the dataset provided for the analysis was considerably smaller than the treatment is typically applied to, there were enough novel elements for the model to have some level of predictive power from its fitting attempts. The width of the ellipses provides an additional reinforcement, as a narrower

short axis presented around the clustered is indicative of a better fit by subsequent orthogonal regression fit lines.

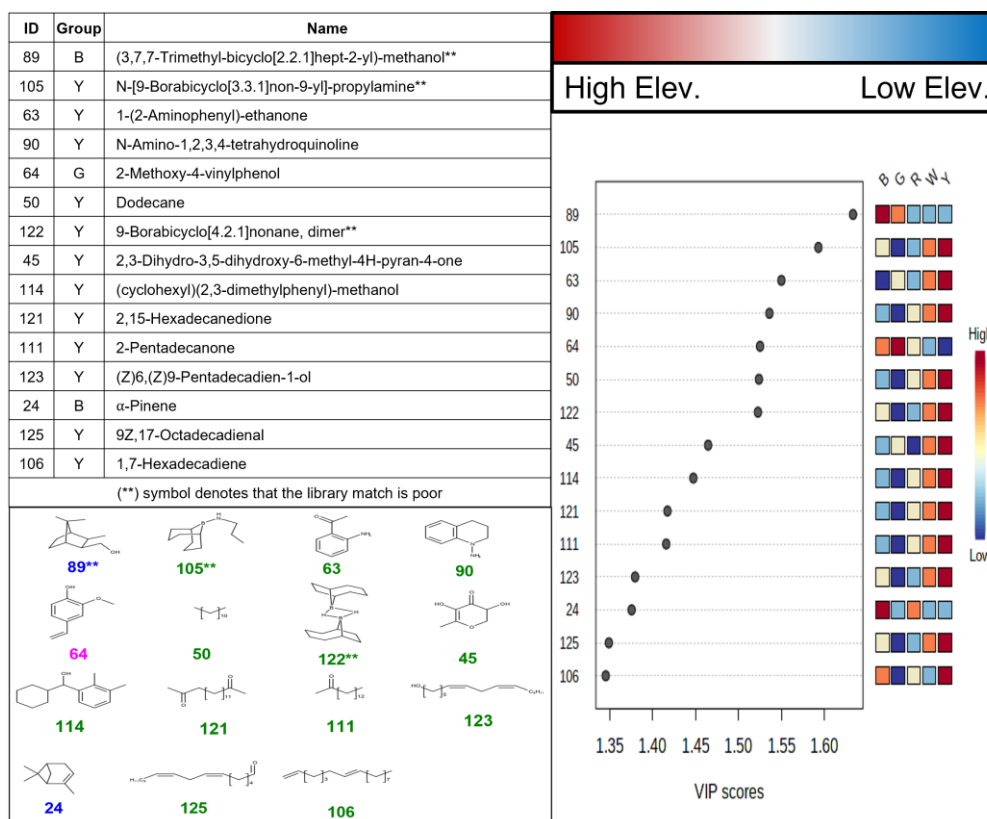


Figure 4. Top 15 VIP compounds from PLS-DA for HS/SPME of Red (R), White (W), Yellow (Y, green), Blue (B, blue), and Waxy Dent (G, pink) dry maize samples. ID label color for structures correspond to the maize species they present the greatest elevation (Elev.) in.

The PLS-DA treatment however, given its forced grouping by varietal, offers a greater degree of differentiation. The VIP compounds identified by this treatment (Fig. 3, supplementary Tables S5-S9) again show a higher number of differentiating compounds for the Y and G sets, contrasted with the PCA output. However, a larger degree of separatory compounds is seen with the B set, and the R set shows a novel response for dimethyl sulfide, where the PCA model produced a much lower differentiating power for these species. These differences are visually apparent in their chromatograms (Fig. 2, supplementary Fig. S1), with lower abundance species more visible for the B set after $t_R=35$ min. Additionally, the R was observed to be the only varietal to show a pronounced abundance of dimethyl sulfide (ID#2, $t_R=6.355$ min, Fig. 2 & Fig. S1). Dimethyl sulfide has been identified in fermented foods, wines, and beers, contributing both positive and negative sensory characteristics, dependent on the medium and the concentration^{52,53}. Generation of volatile sulfur compounds in wine has been attributed

to bacterial and yeast activity⁵², the former seeming to be more likely here, though wild yeast is considered ubiquitous as well.

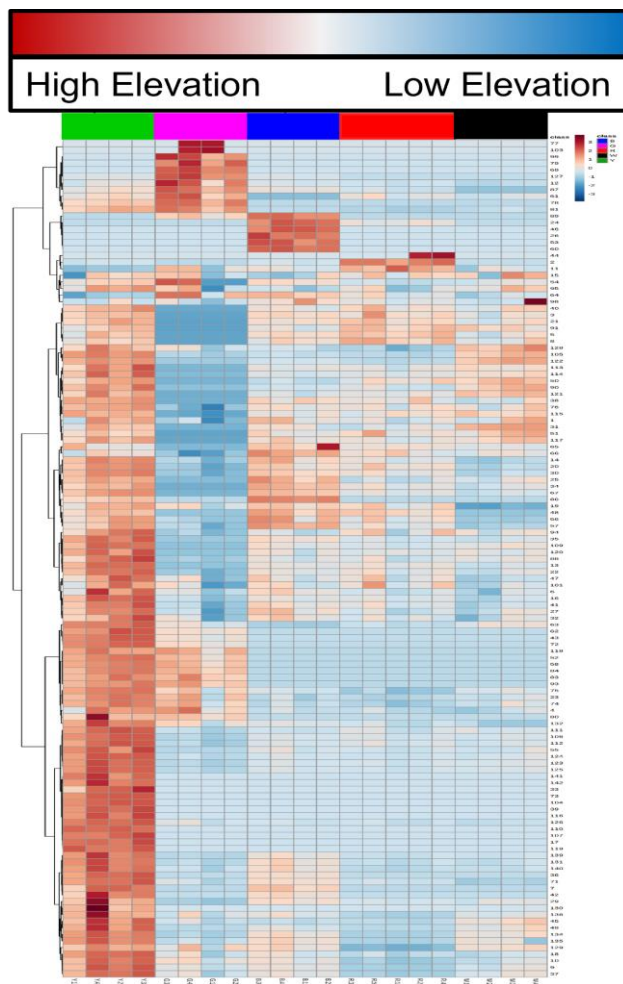


Figure 5. Condensed PLS-DA generated heat map indicating the differentiating power, or elevation of each compound ID within the species group, separated in vertical columns, indicated by their column header color in parentheses. From left to right: Yellow (green), Yellow Waxy Dent (pink), Blue (blue), Red (red), and White (black) maize species. Full compound list is given in supplementary Table S4. Enlarged heat map is given as supplementary Figure S2 for visibility.

The PLS-DA heat map (Figs. 4, S2) visualizes the high differentiability of the Y cultivar, as seen by the majority of the high elevation compounds attributed to it. Conversely, the R cultivar was determined to have an overall low magnitude for the selected compounds' elevation, but again to the exception of the dimethyl sulfide. Isomers of ionone, both α and β , were identified (ID#78, tR=34.820 min., Fig. S1) most prominently in the Y and G samples and correspond to carotenoid derivatives⁵⁴. Specifically, these compounds have been reported to show a strong correlation to the yellow color of the maize and can have an increased concentration based on the time harvested⁵⁴. This is

contrasted with the R and B samples, whose observed profiles did not appear to contain species attributed to their color differences. The lack of color-contributing species in the R and B samples' HS and the volatile component of the liquid injected suggest further sample preparation, to include extractions, is necessary to isolate and characterize the semi-volatiles and non-volatiles attributable to the color differentiation. A prominent candidate for this would be anthocyanins, which have been previously reported^{55,56}; however, these are typically of lower natural abundance than carotenoids, which also readily impart pigmentation. Additionally, anthocyanins are not readily amenable to the HS sampling methods used in this current study and would require additional processing steps (e.g. derivatization) in order to apply our method to moderate efficacy; they are more often characterized by high pressure liquid chromatography (HPLC). Terpene and terpenoid identification was more convoluted, as the overlapping fragmentation patterns, co-elutions, and protracted stationary phase interactions combined to obfuscate differentiable identifiers for all but the most abundant species, namely furans and furanones.

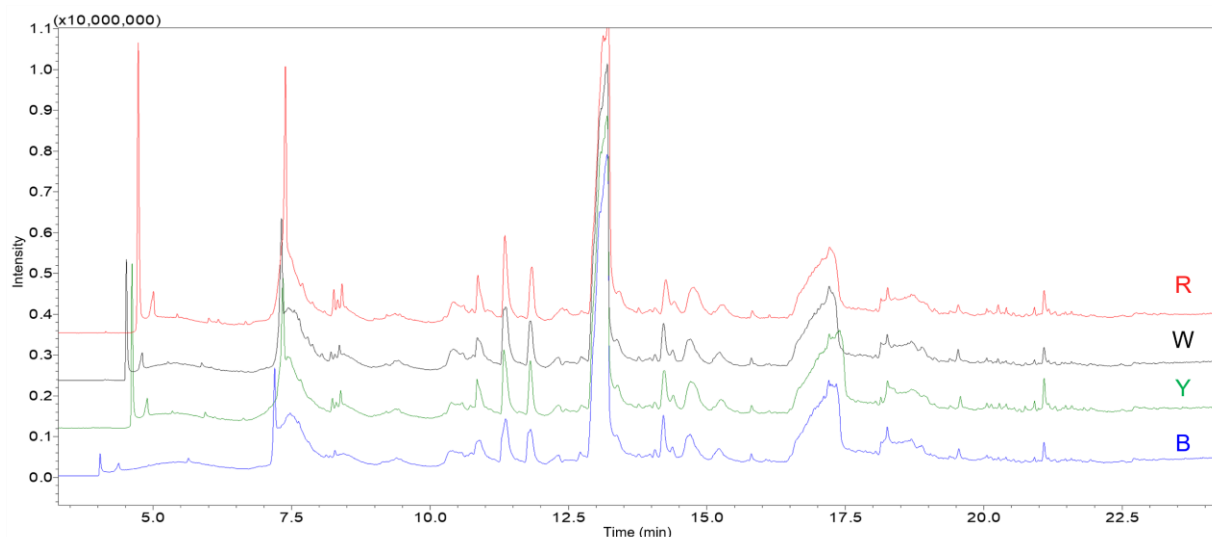


Figure 6. Chromatograms of liquid injection of Red (R), White (W), Yellow (Y), and Blue (B) mash samples. Enlarged version is given as supplementary Figure S3.

Liquid injection proved a poor sample introduction method, as exhibited by the substandard chromatography for a number of the compounds for the R, W, B, and Y beer (Fig. 6, supplementary Fig. S3) and mash (Fig. 7, supplementary Fig. S4) samples. Additionally, a residue was apparent within the glass liner of the injection port, appearing to be a deposit of the nonamenable components present within the sample matrices. This residue was most probably proteins, oligo- or remaining polysaccharides, other macromolecules, or some combination thereof, as the R, W, B, and Y mash and beer samples were not subjected to any sample cleanup procedures as an initial effort to maximize the limited resource.

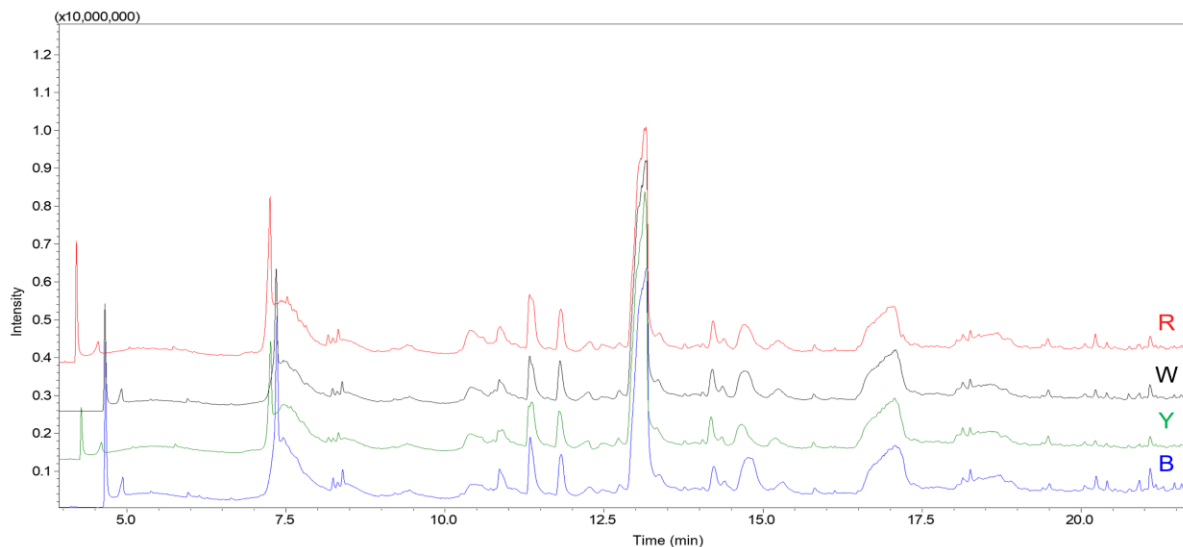


Figure 7. Chromatograms of liquid injection of Red (R), White (W), Yellow (Y), and Blue (B) beer samples. Enlarged version is given as supplementary Figure S5.

In the four beer run analyses performed by liquid injection, glycerol is identified (Fig. 7, tR: 9.0-12.0 min. and supplementary Fig. S4, region 2) as a prominent component, and consequentially, a prominent impediment to efficacy. Glycerol is a known byproduct of yeast metabolism in the production of ethanol via glycolysis^{57,58}, and typically exists in relatively high concentrations, as high as 4 g L⁻¹⁵⁸. The interference presented as a protracted, strongly fronting peak indicative of overload, as well as disturbing the proximal chromatography, seen as variable retention times and abundance for the glycerol itself, in addition to numerous signals throughout the rest of the chromatogram (supplementary Fig. S4, regions 1-4). This gave rise to an additional complication, just as with the liquid mash data, in that the lack of reproducibility precluded the use of PCA or PLS-DA treatments. The glycerol interferences seen with the liquid injections of the four beer samples necessitate further sample preparation prior to additional analyses with HS/SPME-GC/MS, potentially through use of anion exchange chromatography⁵⁹ or solid phase extraction (SPE)⁶⁰. Given the coelution of glycerol with a reduced maltol derivative in higher relative concentration, as well as the potential for stationary phase interference, the ID determinations that were made surrounding this region are more tenuous. Their respective RI's differ by 300, further calling the results into question due to the proximity, particularly for those that showed a lower similarity index. Similar cleanup would be required of the mash samples, were liquid injection sought, in order to mitigate the deposit formation that was observed. The observed residue buildup within the injection port liner could have served as a physical barrier as well; the residue appeared to have occluded as much as 40% of the flow path within the liner.

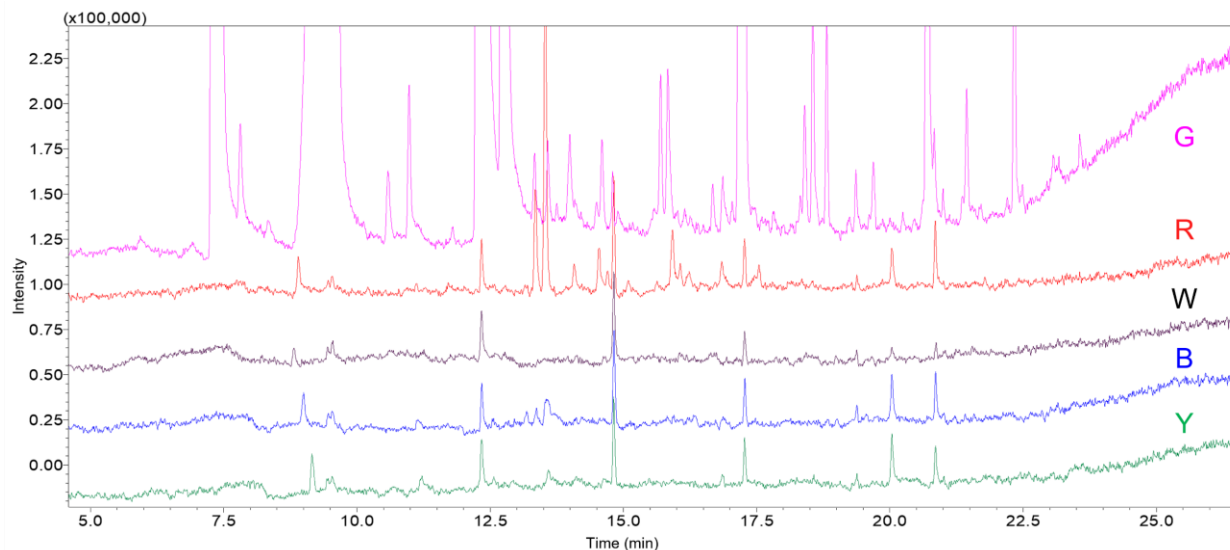


Figure 8. Chromatograms of HS/SPME injection of Waxy Dent (G), Red (R), White (W), Yellow (Y), and Blue (B) mash samples. Enlarged version is given as supplementary Figure S5. Note: the G chromatograms exceed 10^6 in intensity for all peaks off scale.

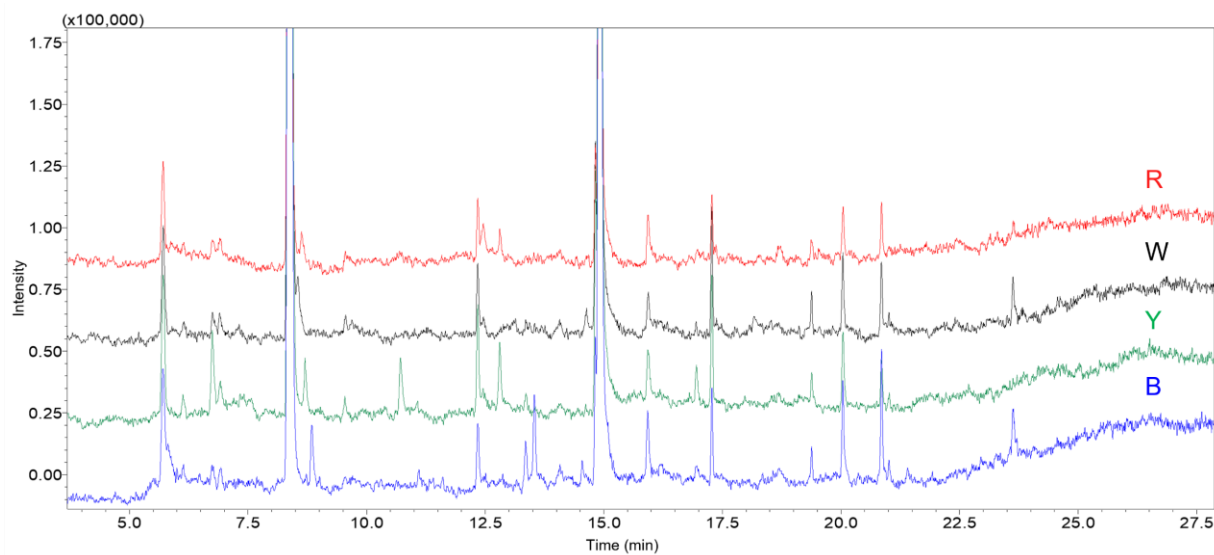


Figure 9. Chromatograms of HS/SPME injection of Red (R), White (W), Yellow (Y), and Blue (B) beer samples. Enlarged version is given as supplementary Figure S6.

The HS/SPME mash and beer samplings (Figs. 7, S5 and Figs. 8, S6, respectively) gave a marked decrease in both the number and intensity of the observed signals, contrasted with the liquid injection method, as simply observed by their intensity axes. This suggests a larger concentration of semi-volatiles present within the samples, warranting additional preparation methods for consideration. The G mash samples were available in an appreciably higher volume, where approximately 2 L of the G mash solution was provided, contrasted with the approximately 4.5 mL of each of the other 4

varietals that was available. The centrifugation step to remove the suspended solids that was able to be applied to the G samples appears to have served as an additional concentration step, as seen in the two orders of magnitude increase in the signal intensity, over the other four for the HS/SPME mash suite analyses. The carotenoids expected to be present exhibit poor thermal stability, and their preemptive isolation, potentially followed by their characterization through a more amenable pathway (e.g. HPLC⁶¹ or analyte derivatization), could allow for a more diverse HS over the sample due to lack of thermal degradation products competing for the space.

Conclusion

The described method for using HS/SPME-GC/MS was shown to be simplistic in execution and has the potential for expansive modularity for species selection and/or elimination. The appearance of a number of known downstream glycolysis and Maillard products (e.g. furans) in the dry maize analyses suggest that, because of the temperature and duration of the In-Ex process, the maize samples appeared to have begun their breakdown into constituents. This process is akin to the formal mashing process, albeit it appeared to have initiated absent the α -amylase introduction typical to mashing. The pseudo-“dry mashing” period appears to have potentially generated and volatilized a broader array of compounds than what was expected from sole maize samples^{9,62-65}. The elevated temperatures also appear to have contributed to increases in other derivative formations, such as the multiple furan derivatives identified (Table-S4). Though the screening process, by necessity, produced a number of potential data to assess repeatability of the process, further investigation is merited to rule out potential interferences hitherto not considered. The limitation of sample size precluded some analyses, to include replicates of the R, W, Y, and B mashes and beers, certainly reinforcing the potential for greater profile depth, were the available amounts in sufficient quantity. The method’s modular capability would require little work to expand to other precursor grains (e.g. malted and un-malted barley) for a volatiles focus, as well as being adaptable for direct immersion sampling in a liquid matrix.

References

1. Alcohol, recorded per capita (15+) consumption (in litres of pure alcohol) [https://www.who.int/data/gho/data/indicators/indicator-details/GHO/alcohol-recorded-per-capita-\(15-\)-consumption-\(in-litres-of-pure-alcohol\)](https://www.who.int/data/gho/data/indicators/indicator-details/GHO/alcohol-recorded-per-capita-(15-)-consumption-(in-litres-of-pure-alcohol)) (accessed 2021 -10 -18).
2. United Nations Department of Economic and Social Affairs. *World Population Prospects 2017 - Volume I: Comprehensive Tables*; United Nations, 2021. doi:10.18356/9789210001014.
3. Whisky - Worldwide | Statista Market Forecast <https://www.statista.com/outlook/cmo/alcoholic-drinks/spirits/whisky/worldwide> (accessed 2021 -10 -18).
4. Global Whiskey Market: Global Industry Perspective, Comprehensive Analysis, And Forecast, 2020 – 2026 <https://www.zionmarketresearch.com/report/whiskey-market> (accessed 2020 -10 -08).
5. IBISWorld - Industry Market Research, Reports, and Statistics <https://www.ibisworld.com/default.aspx> (accessed 2021 -11 -02).
6. CFR 5.22, Bureau of Alcohol, Tobacco, Firearms, and Explosives. **2008** <https://www.govinfo.gov/content/pkg/CFR-1998-title27-vol1/pdf/CFR-1998-title27-vol1-part5.pdf> (accessed 2021 -10 -18).
7. A Midwinter Night's Dram, High West Distillery <https://www.highwest.com/products/a-midwinter-nights-dram.php> (accessed 2021 -10 -02).
8. Schrieberg, F. Here Are 10 Weirdly Flavored Whiskies That Actually Exist <https://www.forbes.com/sites/felipeschrieberg/2020/08/23/10-weird-flavored-whiskies/> (accessed 2021 -10 -02).
9. Agu, R. c.; Bringhurst, T. a.; Brosnan, J. m. Production of Grain Whisky and Ethanol from Wheat, Maize and Other Cereals. *J. Inst. Brew.* **2006**, 112 (4), 314–323. doi:10.1002/j.2050-0416.2006.tb00737.x.
10. Ługowoj, S.; Balcerk, M. Traditional and New Raw Materials for Spirit Beverage Production. In *Acta Universitatis Lodzianis. Folia Biologica et Oecologica*; Post Conference Communications and Articles; Lodz University Press: Online, 2021; Vol. 17, pp 70–78. doi:10.18778/1730-2366.16.17.
11. Wright, S.; Pilkington, H. Whiskies of Canada and the United States. In *Whisky and Other Spirits: Technology, Production and Marketing*; Elsevier, 2022; pp 87–104. doi:10.1016/B978-0-12-822076-4.00005-X.
12. Strickland, M.; Wright, S.; Pilkington, H. Craft Distilling in North America. In *Whisky and Other Spirits: Technology, Production and Marketing*; Elsevier, 2022; pp 105–123. doi:10.1016/B978-0-12-822076-4.00021-8.
13. Quinn, D.; Nation, B. Irish Whiskey. In *Whisky and Other Spirits: Technology, Production and Marketing*; Elsevier, 2022; pp 125–136. doi:10.1016/B978-0-12-822076-4.00010-3.
14. Bringhurst, T. A.; Harrison, B. M.; Brosnan, J. Scotch Whisky: Raw Material Selection and Processing. In *Whisky and Other Spirits: Technology, Production and Marketing*; Elsevier, 2022; pp 137–203. doi:10.1016/B978-0-12-822076-4.00018-8.

15. Murray, D. Grain Whisky Distillation. In *Whisky and Other Spirits: Technology, Production and Marketing*; Elsevier, 2022; pp 271–289. doi:10.1016/B978-0-12-822076-4.00001-2.
16. *The Alcohol Textbook*, 4th ed.; Jacques, K. A., Lyons, T. P., Kelsall, D. R., Eds.; Nottingham University Press: Nottingham, 2003.
17. Fukuyo, S.; Myojo, Y. Japanese Whisky. In *Whisky and Other Spirits: Technology, Production and Marketing*; Elsevier, 2022; pp 7–16. doi:10.1016/B978-0-12-822076-4.00020-6.
18. Maitin, B. K. Indian Whiskies. In *Whisky and Other Spirits: Technology, Production and Marketing*; Elsevier, 2022; pp 75–86. doi:10.1016/B978-0-12-822076-4.00027-9.
19. McConnell, M. *Grain Crushings and Co-Products Production 2019 Summary*; Grain Crushings and Co-Products Production; Agriculture Statistics ISSN: 2470-9913; United States Department of Agriculture, 2020; p 7.
20. McConnell, M. *Crop Production 2019 Summary 01/10/2020*; National Agricultural Statistics Service; Agriculture Statistics ISSN: 1057-7823; United States Department of Agriculture, 2020; p 124.
21. McConnell, M. *Feed Yearbook: Report March 13, 2020*; Agriculture Statistics; United States Department of Agriculture, 2020.
22. McConnell, M. *Feed Grains: Yearbook Tables*; Feed Grains Database; Federal Database; United States Department of Agriculture: Washington, D.C., 2021.
23. McConnell, M. Corn and Other Feedgrains - Market Outlook <https://www.ers.usda.gov/topics/crops/corn-and-other-feedgrains/market-outlook/> (accessed 2021 -11 -15).
24. Zhou, S.; Kremling, K. A.; Bandillo, N.; Richter, A.; Zhang, Y. K.; Ahern, K. R.; Artyukhin, A. B.; Hui, J. X.; Younkin, G. C.; Schroeder, F. C.; Buckler, E. S.; Jander, G. Metabolome-Scale Genome-Wide Association Studies Reveal Chemical Diversity and Genetic Control of Maize Specialized Metabolites. *Plant Cell* **2019**, *31* (5), 937–955. doi:10.1105/tpc.18.00772.
25. Arnold, R. J.; Ochoa, A.; Kerth, C. R.; Miller, R. K.; Murray, S. C. Assessing the Impact of Corn Variety and Texas Terroir on Flavor and Alcohol Yield in New-Make Bourbon Whiskey. *PLoS ONE* **2019**, *14* (8), e0220787. doi:10.1371/journal.pone.0220787.
26. *Book II Grain Grading Procedures*; Marketing and Regulatory Programs; Policy Handbook Grain Inspection Handbook II; United States Department of Agriculture: Washington, D.C., 2020; p 355.
27. Lijewski, R. *Moisture Handbook*; Marketing and Regulatory Programs; Policy Handbook; United States Department of Agriculture: Washington, D.C., 2013; p 34.
28. Hellevang, K. J. Grain Drying. NDSU Extension Service November 1994.
29. Will. Grain Drying – Why Do They Do That? *Iowa Agriculture Literacy*, 2015.
30. Hellevang, K. J.; Wilcke, W. F. Maintaining Corn Quality for Wet Milling. NDSU Extension Service September 1996.
31. Wilcke, W.; Morey, R. V. Natural-air corn drying <https://extension.umn.edu/corn-harvest/natural-air-corn-drying> (accessed 2020 -04 -18).

32. Asemu, A. M.; Habtu, N. G.; Delele, M. A.; Subramanyam, B.; Alavi, S. Drying Characteristics of Maize Grain in Solar Bubble Dryer. *J. Food Process Eng.* **2019**, *43* (2), e13312. doi:10.1111/jfpe.13312.
33. Câmara, J. S.; Alves, M. A.; Marques, J. C. Development of Headspace Solid-Phase Microextraction-Gas Chromatography–Mass Spectrometry Methodology for Analysis of Terpenoids in Madeira Wines. *Anal. Chim. Acta* **2006**, *555* (2), 191–200. doi:10.1016/j.aca.2005.09.001.
34. Perez-Olivero, S. J.; Perez-Pont, M. L.; Conde, J. E.; Perez-Trujillo, J. P. Determination of Lactones in Wines by Headspace Solid-Phase Microextraction and Gas Chromatography Coupled with Mass Spectrometry. *J. Anal. Meth. Chem.* **2014**, *2014*. doi:10.1155/2014/863019.
35. Rodríguez-Bencomo, J. J.; Conde, J. E.; García-Montelongo, F.; Pérez-Trujillo, J. P. Determination of Major Compounds in Sweet Wines by Headspace Solid-Phase Microextraction and Gas Chromatography. *J. Chromatogr. A* **2003**, *991* (1), 13–22. doi:10.1016/S0021-9673(03)00211-5.
36. Wu, Y. V.; Payne-Wahl, K. L.; Vaughn, S. F. Analysis of Headspace Volatiles of Corn Gluten Meal. *Cereal Chem.* **2003**, *80* (5), 567–569. doi:10.1094/CCHEM.2003.80.5.567.
37. Lucca, A. J. D.; Boué, S. M.; Carter-Wientjes, C.; Bhatnagar, D. Volatile Profiles and Aflatoxin Production by Toxigenic and Non-Toxigenic Isolates of *Aspergillus Flavus* Grown on Sterile and Non-Sterile Cracked Corn. *Ann. Agric. Environ. Med.* **2012**, *19* (1), 8.
38. Caldeira, M.; Rodrigues, F.; Perestrelo, R.; Marques, J. C.; Câmara, J. S. Comparison of Two Extraction Methods for Evaluation of Volatile Constituents Patterns in Commercial Whiskeys Elucidation of the Main Odour-Active Compounds. *Talanta* **2007**, *74* (1), 78–90. doi:10.1016/j.talanta.2007.05.029.
39. Demyttenaere, J.; Sanchezmartinez, J.; Verhe, R.; Sandra, P.; Dekimpe, N. Analysis of Volatiles of Malt Whisky by Solid-Phase Microextraction and Stir Bar Sorptive Extraction. *J. Chromatogr. A* **2003**, *985* (1–2), 221–232. doi:10.1016/S0021-9673(02)01471-1.
40. Fitzgerald, G.; James, K. J.; MacNamara, K.; Stack, M. A. Characterisation of Whiskeys Using Solid-Phase Microextraction with Gas Chromatography–Mass Spectrometry. *J. Chromatogr. A* **2000**, *896* (1–2), 351–359. doi:10.1016/S0021-9673(00)00737-8.
41. Phetxumphou, K.; Miller, G.; Ashmore, P. L.; Collins, T.; Lahne, J. Mashbill and Barrel Aging Effects on the Sensory and Chemometric Profiles of American Whiskeys: Mashbill and Barrel Aging Effects on the Sensory and Chemometric Profiles of American Whiskeys. *J. Inst. Brew.* **2020**, *126* (2), 194–205. doi:10.1002/jib.596.
42. Jeleń, H. H.; Majcher, M.; Szwengiel, A. Key Odorants in Peated Malt Whisky and Its Differentiation from Other Whisky Types Using Profiling of Flavor and Volatile Compounds. *LWT* **2019**, *107*, 56–63. doi:10.1016/j.lwt.2019.02.070.
43. Wiśniewska, P.; Dymerski, T.; Wardencki, W.; Namieśnik, J. Chemical Composition Analysis and Authentication of Whisky. *J. Sci. Food Agric.* **2021**, *95* (11), 2159–2166. doi:10.1002/jsfa.6960.

44. Martins, A. R.; Talhavini, M.; Vieira, M. L.; Zacca, J. J.; Braga, J. W. B. Discrimination of Whisky Brands and Counterfeit Identification by UV–Vis Spectroscopy and Multivariate Data Analysis. *Food Chem.* **2017**, *229*, 142–151. doi:10.1016/j.foodchem.2017.02.024.
45. Aylott, R. Whisky Analysis. In *Whisky and Other Spirits*; Elsevier, 2022; pp 335–362. doi:10.1016/B978-0-12-822076-4.00009-7.
46. Salo, P. Determining the Odor Thresholds for Some Compounds in Alcoholic Beverages. *J. Food Sci.* **1970**, *35* (1), 95–95. doi:https://doi.org/10.1111/j.1365-2621.1970.tb12378.x.
47. Facts & Figures <https://www.scotch-whisky.org.uk/insights/facts-figures/> (accessed 2021 -11 -29).
48. Youmans, M. Clarkson Grain Company. Cerro Gordo, IL. Personal Communication, 2021.
49. Lee, M. L.; Vassilaros, D. L.; White, C. M. Retention Indices for Programmed-Temperature Capillary-Column Gas Chromatography of Polycyclic Aromatic Hydrocarbons. *Anal. Chem.* **1979**, *51* (6), 768–773. doi:10.1021/ac50042a043.
50. Pang, Z.; Chong, J.; Zhou, G.; de Lima Morais, D. A.; Chang, L.; Barrette, M.; Gauthier, C.; Jacques, P.-É.; Li, S.; Xia, J. MetaboAnalyst 5.0: Narrowing the Gap between Raw Spectra and Functional Insights. *Nucleic Acids Res.* **2021**, *49* (W1), W388–W396. doi:10.1093/nar/gkab382.
51. Aylott, R. I.; Clyne, A. H.; Fox, A. P.; Walker, D. A. Analytical Strategies to Confirm Scotch Whisky Authenticity. *Analyst* **1994**, *119* (8), 1741–1746. doi:10.1039/an9941901741.
52. Landaud, S.; Helinck, S.; Bonnarne, P. Formation of Volatile Sulfur Compounds and Metabolism of Methionine and Other Sulfur Compounds in Fermented Food. *Appl. Microbiol. Biotechnol.* **2008**, *77* (6), 1191–1205. doi:10.1007/s00253-007-1288-y.
53. Swiegers, J. H.; Pretorius, I. S. Modulation of Volatile Sulfur Compounds by Wine Yeast. *Appl. Microbiol. Biotechnol.* **2007**, *74* (5), 954–960. doi:10.1007/s00253-006-0828-1.
54. Gallon, C. Z.; Fuller, S. C.; Fanning, K. J.; Smyth, H. E.; Pun, S.; Martin, I. F.; O'Hare, T. J. Increase in β -Ionone, a Carotenoid-Derived Volatile in Zeaxanthin-Biofortified Sweet Corn. *J. Agric. Food Chem.* **2013**, *61* (30), 7181–7187. doi:10.1021/jf402326e.
55. Cevallos-Casals, B. A.; Cisneros-Zevallos, L. Stability of Anthocyanin-Based Aqueous Extracts of Andean Purple Corn and Red-Fleshed Sweet Potato Compared to Synthetic and Natural Colorants. *Food Chem.* **2004**, *86* (1), 69–77. doi:10.1016/j.foodchem.2003.08.011.
56. Li, Q.; Somavat, P.; Singh, V.; Chatham, L.; Gonzalez de Mejia, E. A Comparative Study of Anthocyanin Distribution in Purple and Blue Corn Coproducts from Three Conventional Fractionation Processes. *Food Chem.* **2017**, *231*, 332–339. doi:10.1016/j.foodchem.2017.03.146.
57. Guo, Z.; Zhang, L.; Ding, Z.; Shi, G. Minimization of Glycerol Synthesis in Industrial Ethanol Yeast without Influencing Its Fermentation Performance. *Metab. Eng.* **2011**, *13* (1), 49–59. doi:10.1016/j.ymben.2010.11.003.

58. Klopper, W. J.; Angelino, S. A. G. F.; Tuning, B.; Vermeire, H. A. Organic Acids and Glycerol in Beer. *J. Inst. Brew.* **1986**, 92 (3), 225–228. doi:10.1002/j.2050-0416.1986.tb04405.x.
59. Zager, S. E.; Doody, T. C. Glycerol Removal from Aqueous Solutions by Anion Exchange. *Ind. Eng. Chem.* **1951**, 43 (5), 1070–1073. doi:10.1021/ie50497a021.
60. Moreira, B. M.; Cunha, J. N. da; Paiva, V. M.; Honório, G. G.; Tarley, R. T.; D’Elia, E. Determination of Free Glycerol in Biodiesel by Molecularly Imprinted Polymer – Based Solid-Phase Extraction (SPE) Using an Enzymatic Spectrophotometric Assay. *Anal. Lett.* **2021**, 54 (10), 1654–1667. doi:10.1080/00032719.2020.1821040.
62. Vanbeneden, N.; Gils, F.; Delvaux, F.; Delvaux, F. R. Variability in the Release of Free and Bound Hydroxycinnamic Acids from Diverse Malted Barley (*Hordeum Vulgare* L.) Cultivars during Wort Production. *J. Agric. Food Chem.* **2007**, 55 (26), 11002–11010. doi:10.1021/jf072340a.
63. Tauer, A.; Elss, S.; Frischmann, M.; Tellez, P.; Pischetsrieder, M. Influence of Thermally Processed Carbohydrate/Amino Acid Mixtures on the Fermentation by *Saccharomyces Cerevisiae*. *J. Agric. Food Chem.* **2004**, 52 (7), 2042–2046. doi:10.1021/jf034995r.
64. Phetxumphou, K.; Miller, G.; Ashmore, P. L.; Collins, T.; Lahne, J. Mashbill and Barrel Aging Effects on the Sensory and Chemometric Profiles of American Whiskeys. *J. Inst. Brew.* **2020**, 126 (2), 194–205. doi:10.1002/jib.596.
65. Ochoa, A. Aroma in New Make Whiskey Determined by Maize Variety and Origin. Master of Science Thesis, Texas A&M University, College Station, Texas, USA, **2017**

Supplemental Information

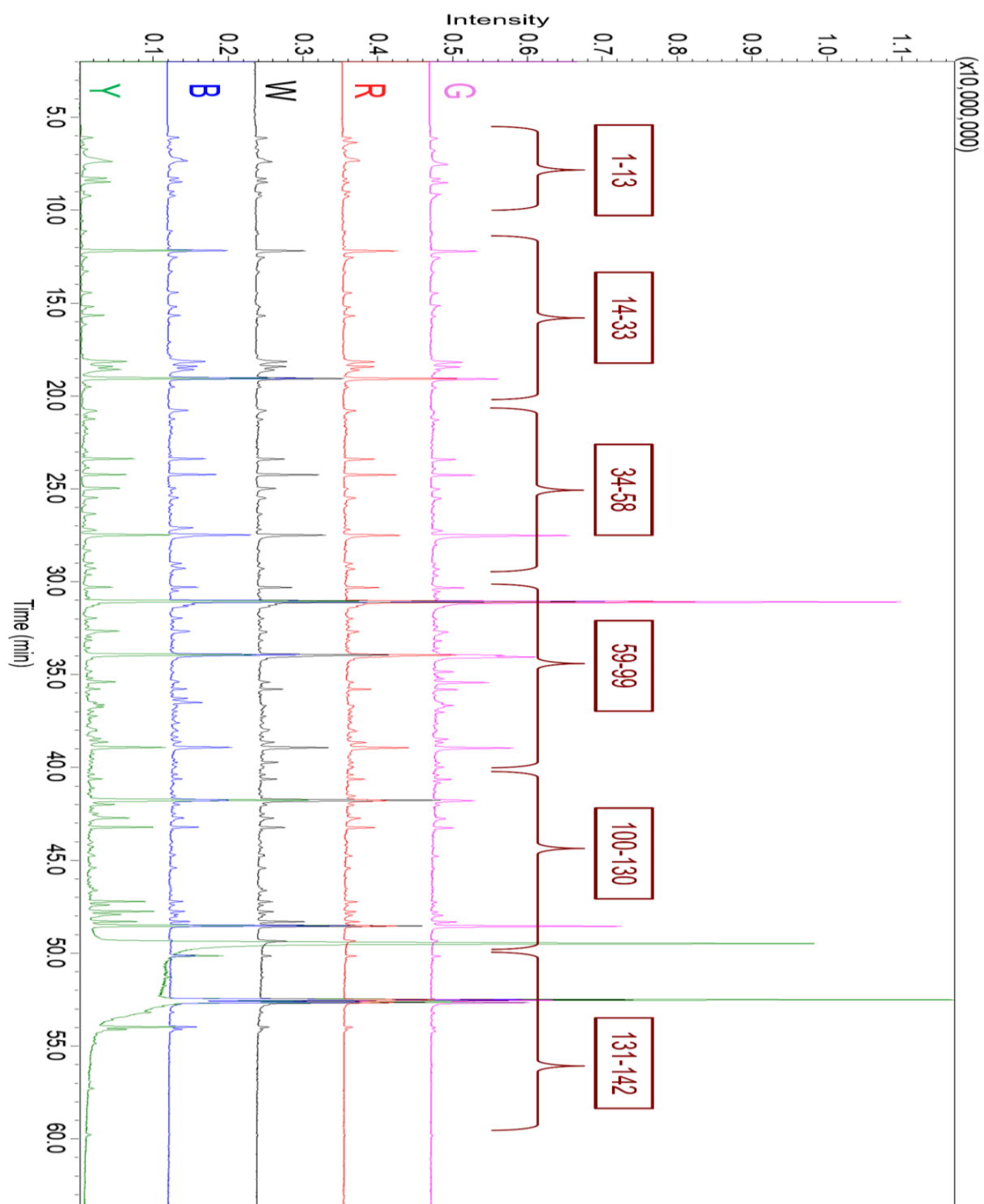


Figure S1. HS/SPME of Waxy Dent (G), Red (R), White (W), Blue (B), and Yellow (Y) dry maize samples, enlarged, with ID ranges. (n=4)

Table S1. Compound ID's, ordered for PLS-DA heat map, for Dry Corn HS/SPME sampling PCA and PLS-DA treatments. (** indicates poor (<80%) Similarity Index with Library)

ID	Name
77	2,4,7,9-Tetramethyl-5-decyn-4,7-diol
103	2,4,7,9-Tetramethyl-5-decyn-4,7-diol
9	3-Methylbutanal
79	2-Methylene-4,8,8-trimethyl-4-vinyl-bicyclo[5.2.0]nonane
69	8-Methylnonanoic acid
127	Unknown 3
12	Pentanal
87	Pentadecane
61	3-Methyl-benzonitrile
78	α/β -Ionone
81	<i>trans</i> -Geranylacetone
89	(3,7,7-Trimethyl-bicyclo[2.2.1]hept-2-yl)-methanol**
24	α -Pinene
46	<i>trans</i> -Verbenol
26	4-Methylene-1-(1-methylethyl)-bicyclo[3.1.0]hex-2-ene
53	2-Hydroxy-6-methyl-benzaldehyde
60	Tridecane
44	Decamethylcyclopentasiloxane
2	Dimethyl sulfide
11	2-Chloro-2-nitropropane
15	Toluene
54	2,3-Dihydro-benzofuran
95	5,6-Dihydro-4-(2,3-dimethyl-2-buten-1-yl)-2H-pyran-2-one
64	2-Methoxy-4-vinylphenol
98	2,2,4-trimethyl-3-carboxyisopropyl-pentanoic acid isobutyl ester
40	5-Ethyl-2-methyl-octane
3	Methylene chloride
21	2-Butylfuran
91	2,6,11-Trimethyl-dodecane
5	n-Hexane
8	Methylcyclopentane
128	<i>trans</i> -Geranylgeraniol
105	N-[9-Borabicyclo[3.3.1]non-9-yl]-propylamine**
122	9-Borabicyclo[4.2.1]nonane, dimer**
113	(2 <i>R</i> ,3 <i>R</i> ,4 <i>aR</i> ,5 <i>S</i> ,8 <i>aS</i>)-2-Hydroxy-4 <i>a</i> ,5-dimethyl-3-(prop-1-en-2-yl)-2,3,4,4 <i>a</i> ,5,6-hexahydronaphthalen-1(8 <i>aH</i>)-one
114	(Cyclohexyl)(2,3-dimethylphenyl)-methanol,
50	Dodecane

ID	Name
90	N-Amino-1,2,3,4-tetrahydroquinoline
121	2,15-Hexadecanedione
38	3,7-Dimethyl-3,6-octadienal
76	Vanillin
115	<i>trans</i> -(<i>Z</i>)- α -Bisabolene epoxide
1	Acetone
31	1,5,5-Trimethyl-6-methylene-cyclohexene
51	Decanal
117	2,5,5,8a-Tetramethyl-6,7,8,8a-tetrahydro-5H-chromen-3-one
65	4-Ethylcyclohexanol
66	3-(2-Methoxyphenyl)propionic acid
14	1-Pentanol
20	2-Heptanone
30	2-Pentylfuran
25	2(<i>E</i>)-Heptenal
34	3-Ethyl-2-methyl-1,3-Hexadiene
67	4(<i>E</i>)-Decenal
86	1-Pentadecene
19	1-Hexanol
48	1,2,3,5,8,8a-Hexahydro-naphthalene
56	Nonanoic acid
57	10-Methylundec-3-en-4-olide
94	Dodecanoic acid
35	3,5-Octadien-2-ol
109	Caryophyllene oxide**
120	5,9,13-Trimethyl-4,8,12-tetradecatrien-1-ol
88	2,4-Di- <i>tert</i> -butylphenol
13	2-Ethylfuran
22	Heptanal
47	Octanoic acid
101	Tetradecanal
6	Acetic acid
16	Hexanal
41	Nonanal
27	Benzaldehyde
32	Octanal
63	1-(2-Aminophenyl)-ethanone
62	4-(2-Hydroxy-2,6,6-trimethylcyclohexyl)-3-buten-2-one
43	2,6-Dimethylcyclohexanol
72	1(<i>E</i>)-(2,3,6-Trimethylphenyl)buta-1,3-diene (TPB, 1)
118	2(<i>Z</i>),13(<i>E</i>)-Octadecadien-1-ol

ID	Name
52	1-Carboxaldehyde-2,6,6-trimethyl-1,3-cyclohexadiene
58	(1S,2S,4S)-trihydroxy- <i>p</i> -Menthane
84	4-(2,6,6-Trimethyl-1-cyclohexen-1-yl)-3-buten-2-one
83	4-(2,6,6-Trimethylcyclohexa-1,3-dienyl)but-3-en-2-one
93	5,6,7,7a-Tetrahydro-4,4,7a-trimethyl-2(4H)-benzofuranone
75	(1.α.,2.α.,3.α.)-2-methyl-3-(1-methylethenyl)-cyclohexanol
23	2,5-Dimethylpyrazine
74	2-Hydroxy-1,1,10-trimethyl-6,9-epidioxydecalin
4	Isobutylene epoxide
80	4-(2,6,6-Trimethyl-1-cyclohexen-1-yl)-2-butanone
132	2-Ethyl-2-methyl-tridecanol
111	2-Pentadecanone
106	1,7-Hexadecadiene
112	1-Pentadecanal
55	Benzeneacetic acid
124	Hexadecyloxirane
123	6(<i>Z</i>), 9(<i>Z</i>)-Pentadecadien-1-ol
125	9(<i>Z</i>),17-Octadecadienal
141	Eicosane
142	1-Iodo-eicosane
33	5-Methyl-3-hepten-2-one
73	2-Butyl-2-octenal
104	6,11-Dimethyl-2,6,10-dodecatrien-1-ol
39	1-Nonen-4-ol
116	6(<i>Z</i>),9(<i>Z</i>)-Pentadecadien-1-ol
126	14-Methyl-8-hexadecenal
110	4-(5-Hydroxy-2,6,6-trimethyl-1-cyclohexen-1-yl)-3-buten-2-one
107	8-Heptadecene
17	Methylpyrazine
119	Unknown 2
139	Linoleyl acetate
131	Hexadecanoic acid ethyl ester
140	9(<i>E</i>)-Octadecenoic acid ethyl ester
36	1-Nitrohexane
71	5-Hexyldihydro-2(3H)-furanone
7	Ethyl Acetate
42	Maltol
29	Methyl-4- <i>tert</i> -butoxy-3-hydroxybutanoate
130	n-Hexadecanoic acid
136	Cyclopentanetridecanoic acid methyl ester
45	2,3-Dihydro-3,5-dihydroxy-6-methyl-4H-pyran-4-one

ID	Name
49	3,5-Dihydroxy-2-methyl-4H-pyran-4-one
134	10-Octadecynoic acid methyl ester
135	9(Z)-Octadecenoic acid methyl ester
129	Hexadecanoic acid methyl ester
18	Furfural
10	2-Methylbutanal
9	3-Methylbutanal
37	Benzeneacetaldehyde

Table S2. VIP Compounds for Waxy Dent (G) dry maize, (-) denotes absence is descriptive (** indicates poor (<80%) Similarity Index with Library)

ID (G)	Name
77	2,4,7,9-Tetramethyl-5-decyn-4,7-diol
103	2,4,7,9-Tetramethyl-5-decyn-4,7-diol
99	Unknown 1
79	2-Methylene-4,8,8-trimethyl-4-vinyl-bicyclo[5.2.0]nonane
69	8-Methylnonanoic acid
127	Unknown 3
12	Pentanal
87	Pentadecane
61	3-Methyl-benzonitrile
78	α/β -Ionone
81	<i>trans</i> -Geranylacetone
89	(3,7,7-Trimethyl-bicyclo[2.2.1]hept-2-yl)-methanol**
40	5-Ethyl-2-methyl-octane
-3	Methylene chloride
-21	2-Butylfuran
-91	2,6,11-Trimethyl-dodecane
-55	Benzeneacetic acid
-8	Methylcyclopentane

Table S3. VIP Compounds for Yellow (Y) dry maize, (-) denotes absence is descriptive

ID (Y)	Name
111	2-Pentadecanone
106	1,7-Hexadecadiene
112	1-Pentadecanal
55	Benzeneacetic acid

ID (Y)	Name
124	Hexadecyloxirane
123	6(Z),9(Z)-Pentadecadien-1-ol
125	9(Z),17-Octadecadienal
141	Eicosane
142	1-Iodo-eicosane
33	5-Methyl-3-hepten-2-one
73	2-Butyl-2-octenal
104	6,11-Dimethyl-2,6,10-dodecatrien-1-ol
39	1-Nonen-4-ol
116	6(Z),9(Z)-Pentadecadien-1-ol
126	14-Methyl-8-hexadecenal
110	4-(5-Hydroxy-2,6,6-trimethyl-1-cyclohexen-1-yl)-3-buten-2-one
107	8-Heptadecene
17	Methylpyrazine
119	Unknown 2

Table S4. VIP Compounds for Blue (B) dry maize, (-) denotes absence is descriptive (** indicates poor (<80%) Similarity Index with Library)

ID (B)	Name
89	(3,7,7-Trimethyl-bicyclo[2.2.1]hept-2-yl)-methanol**
24	α -Pinene
46	<i>trans</i> -Verbenol
26	4-Methylene-1-(1-methylethyl)-bicyclo[3.1.0]hex-2-ene
53	2-Hydroxy-6-methyl-benzaldehyde
60	Tridecane

Table S5. VIP Compounds for Red (R) dry maize, (-) denotes absence is descriptive

ID (R)	Name
2	Dimethyl sulfide
11	2-Chloro-2-nitropropane

Table S6. VIP Compound for White (W) dry maize, (-) denotes absence is descriptive

ID (W)	Name
-19	1-Hexanol

High Elevation Low Elevation

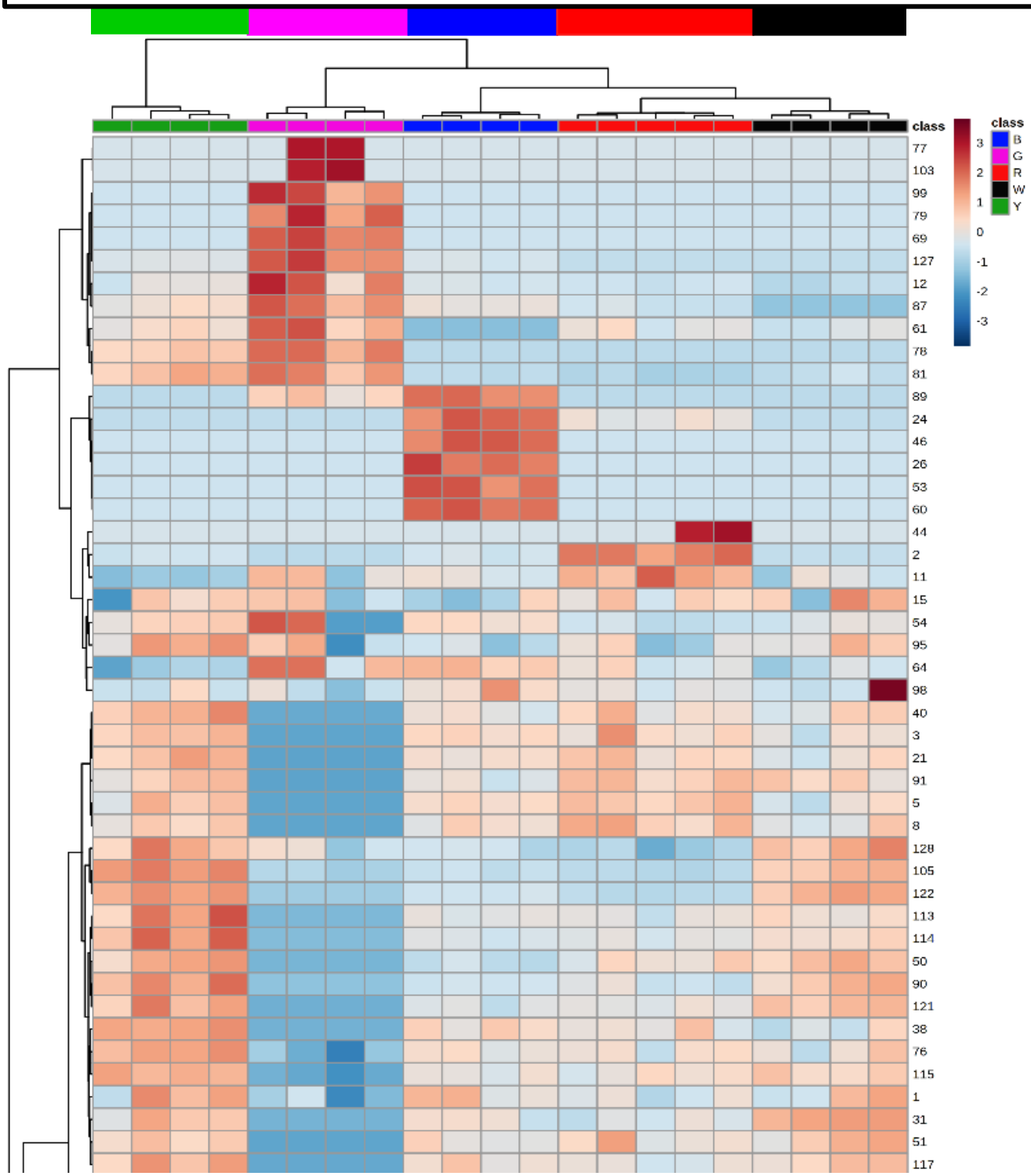


Figure S2. Enlarged PLS-DA heat map for HS/SPME of dry maize samples for each species group, separated in vertical columns, indicated by their column header color in parentheses. From left to right: Yellow (green), Waxy Dent (pink), Blue (blue), Red (red), and White (black) maize species.

High Elevation Low Elevation

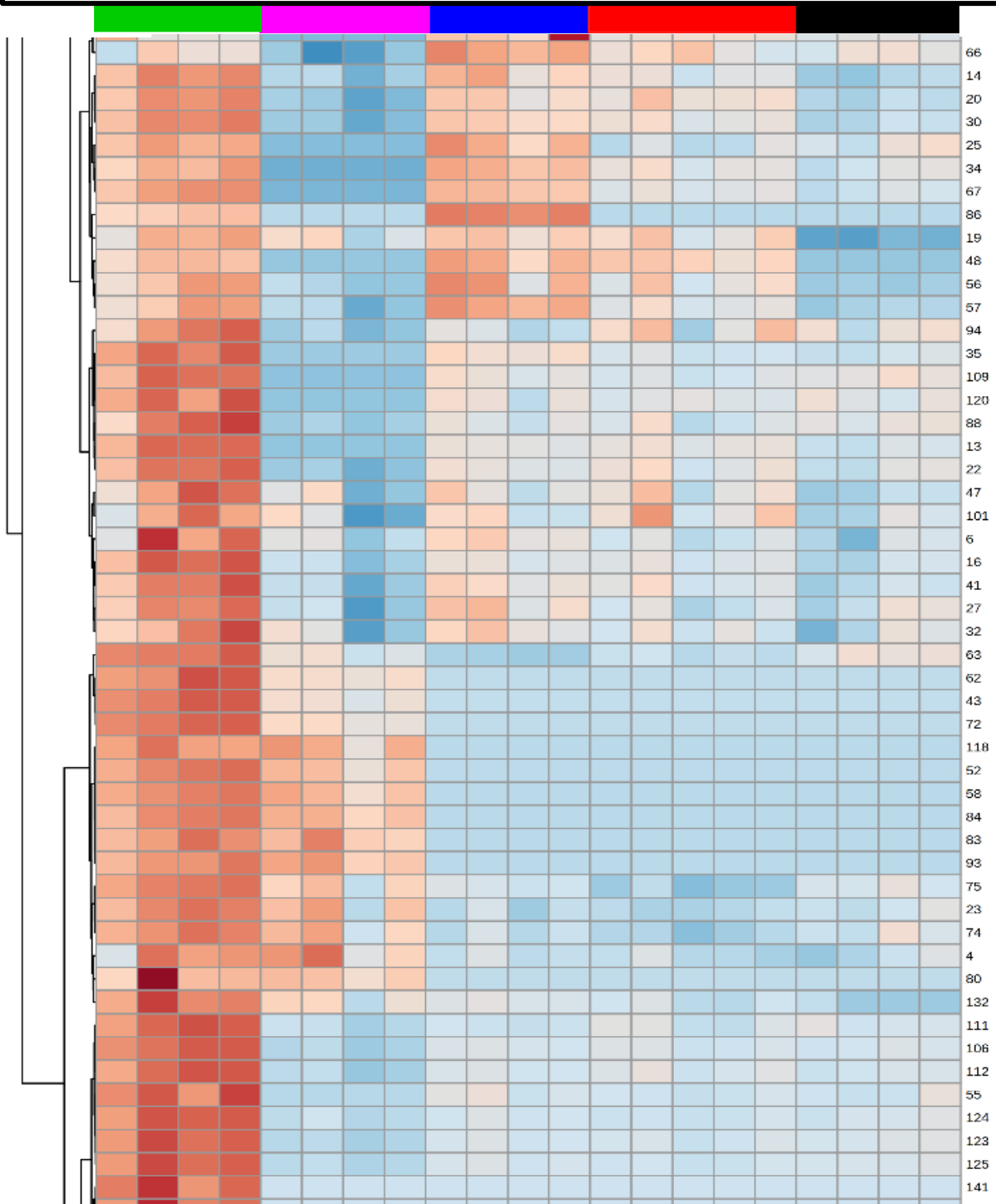


Figure S2 (Continued). Enlarged PLS-DA heat map for HS/SPME of dry maize samples for each species group, separated in vertical columns, indicated by their column header color in parentheses. From left to right: Yellow (green), Waxy Dent (pink), Blue (blue), Red (red), and White (black) maize species.

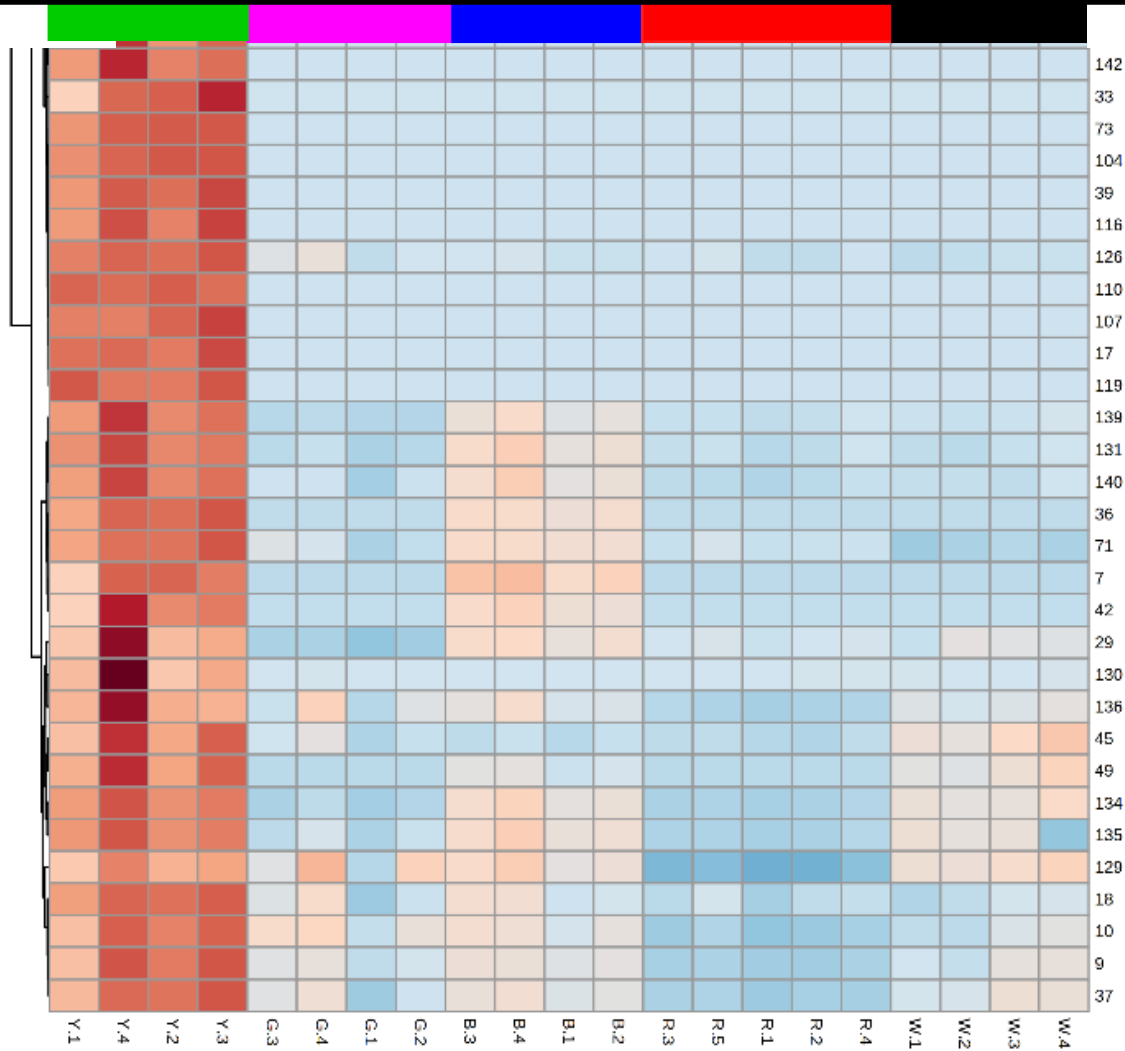
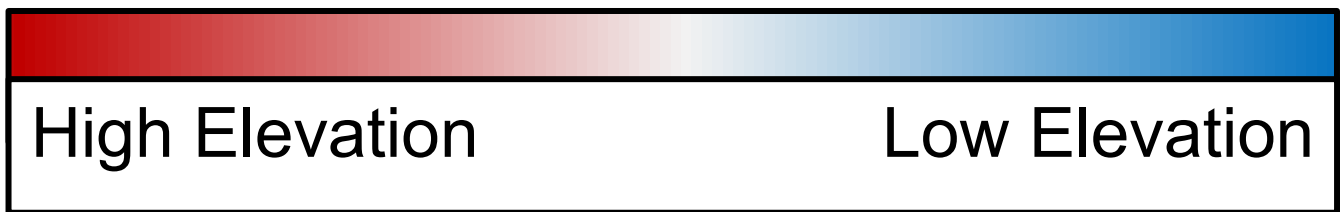


Figure S2 (Continued). Enlarged PLS-DA heat map for HS/SPME of dry maize samples for each species group, separated in vertical columns, indicated by their column header color in parentheses. From left to right: Yellow (green), Waxy Dent (pink), Blue (blue), Red (red), and White (black) maize species.

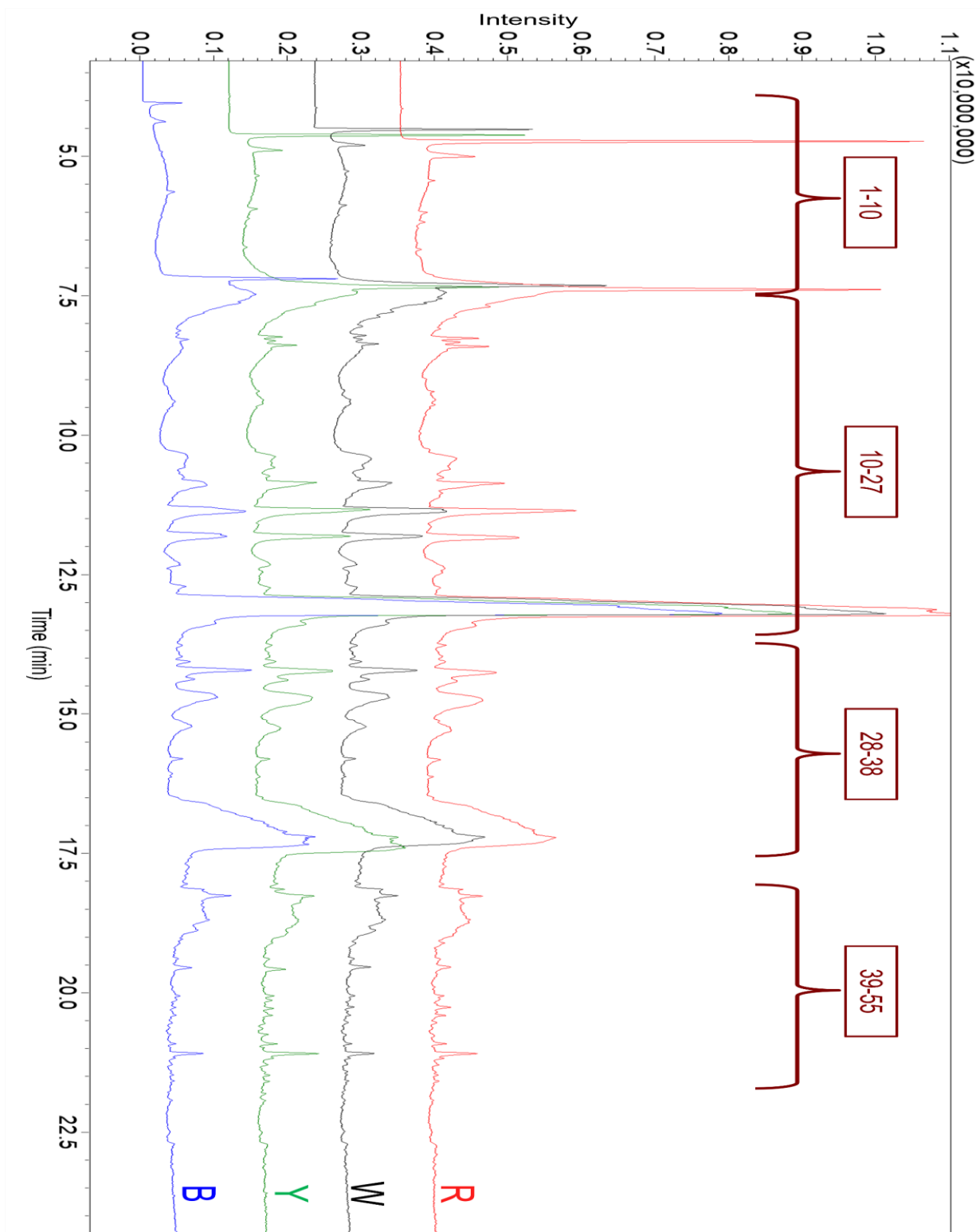


Figure S3. Liquid mash injection chromatograms of Red (R), White (W), Yellow (Y), and Blue (B) mash samples. Compound ID ranges are indicated above their respective retention time ranges.

Table S7. Compound ID's for liquid mash sampling

ID	Name
1	Dimethylsilanediol
2	Formic acid
3	Acetic acid
4	1,2-Propanediol acetate
5	Propylene glycol
6	2-Propenoic acid oxiranylmethyl ester
7	<i>cis</i> -3-Cyclopentene-1,2-diol
8	2-Methyl[1,3,4]oxadiazole
9	2-Furanmethanol
10	3-Furanmethanol
11	2(5H)-Furanone
12	(+)-2(S)-Pyrrolidinemethanol
13	1,2-Cyclopentanedione
14	5-Acetyldihydro-2(3H)-furanone
15	2,4-Dihydroxy-2,5-dimethyl-3(2H)-furan-3-one
16	Isomaltol
17	5-(Hydroxymethyl)dihydrofuran-2(3H)-one
18	3-Furancarboxylic acid
19	Methyl 2-furoate
20	Maltol
21	2,3-Dihydro-3,5-dihydroxy-6-methyl-4H-pyran-4-one
22	3-(Acetylthio)-2(S)-methyl-propanoic acid
23	Catechol
24	5-(1,2-Dihydroxyethyl)dihydrofuran-2-one
25	5-(Hydroxymethyl)dihydrofuran-2(3H)-one
26	5-Hydroxymethylfurfural
27	3-Hydroxy-octanoic acid methyl ester
28	1-(2,5-Dihydroxyphenyl)-ethanone
29	5-Methyl-2-(1-methylethyl)-cyclohexanol
30	5-Acetoxymethyl-2-furaldehyde
31	6-Methyl-2-heptanol acetate
32	2,4-Methylene-D-epirhamnitol
33	2-Hydroxy-3-methylsuccinic acid
34	1,2,3-Benzenetriol
35	2(Z),5(Z)-Dimethyl-2,4-hexadienedioic acid
36	4-Methylcyclohexaneacetic acid
37	1,6-Anhydro- β -D-glucopyranose
38	7-(1-Bromoethyl)-3,3-dimethyl-bicyclo[4.1.0]heptan-2-one**
39	2 γ ,3 γ -Tetramethyl-2-cyclopentene-1-butanal

ID	Name
40	Cirsiumaldehyde
41	Gabapentin N-trifluoroacetate
42	5-[(2-Methylimidazol-1-yl)methyl]furan-2-carboxylic acid
43	3,3'-Sulfonyl- <i>bis</i> -propanoic acid
44	Cirsiumaldehyde
45	Spiroxamine
46	Acetic acid, 3,6-diacetoxy-2,4-dimethyl-tetrahydropyran-4-yl ester
47	15-Octadecenal
48	Fumaric acid, <i>cis</i> -hex-3-enyl heptyl ester
49	Cirsiumaldehyde
50	1,2- <i>bis</i> (4-Amino-3-furazanyloxy)-propane
51	Unknown 1
52	1,2- <i>bis</i> (4-Amino-3-furazanyloxy)-propane
53	Succinic acid, cyclohexylmethyl hex-5-en-1-yl ester
54	Fumaric acid, <i>cis</i> -hex-3-enyl octyl ester
55	2-(2-Hydroxy-cyclohexylamino)-3-(1H-imidazol-4-yl)-propionic acid

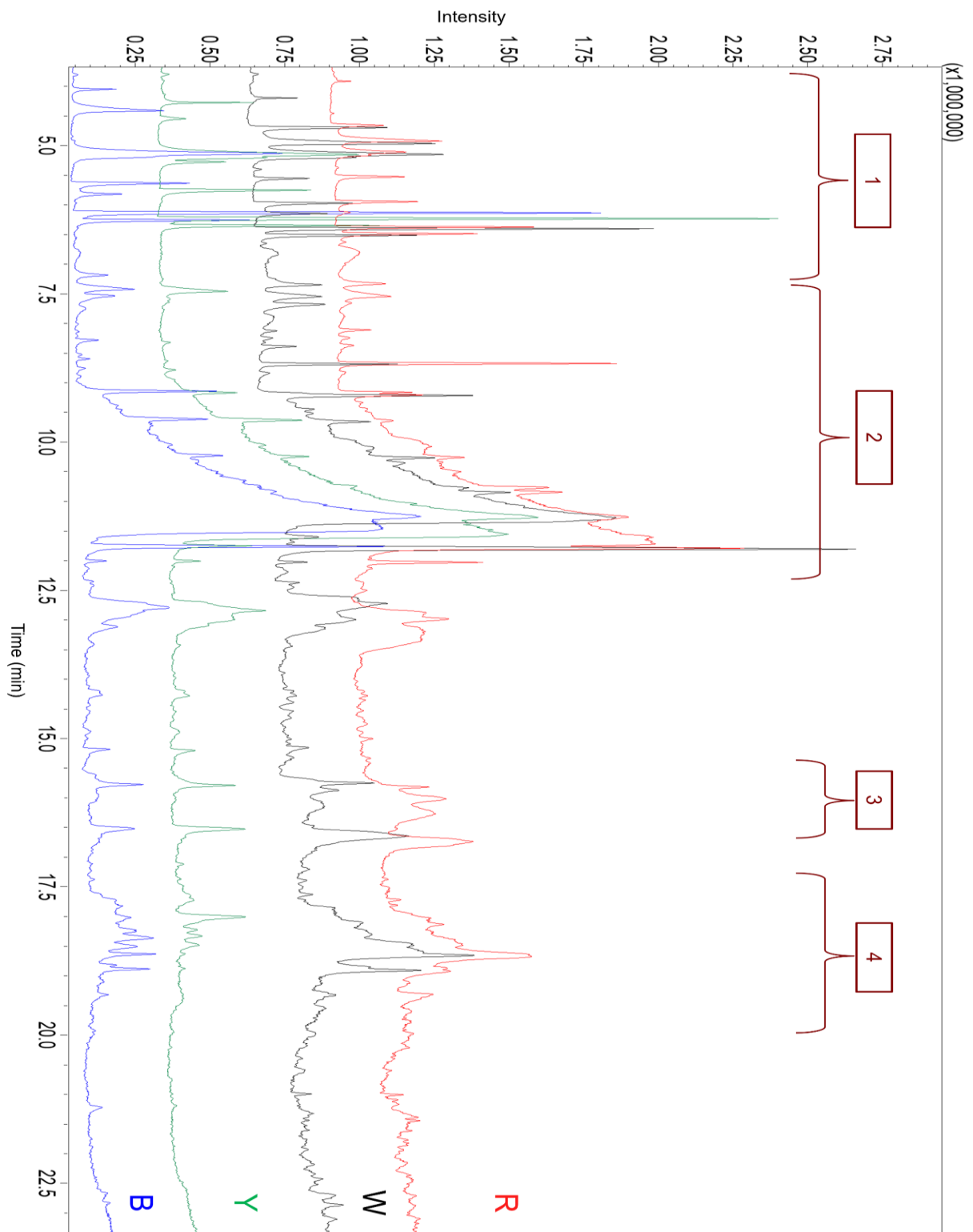


Figure S4. Liquid beer injection chromatograms of Red (R), White (W), Yellow (Y), and Blue (B) beer samples. Brackets indicate 4 regions of interest.

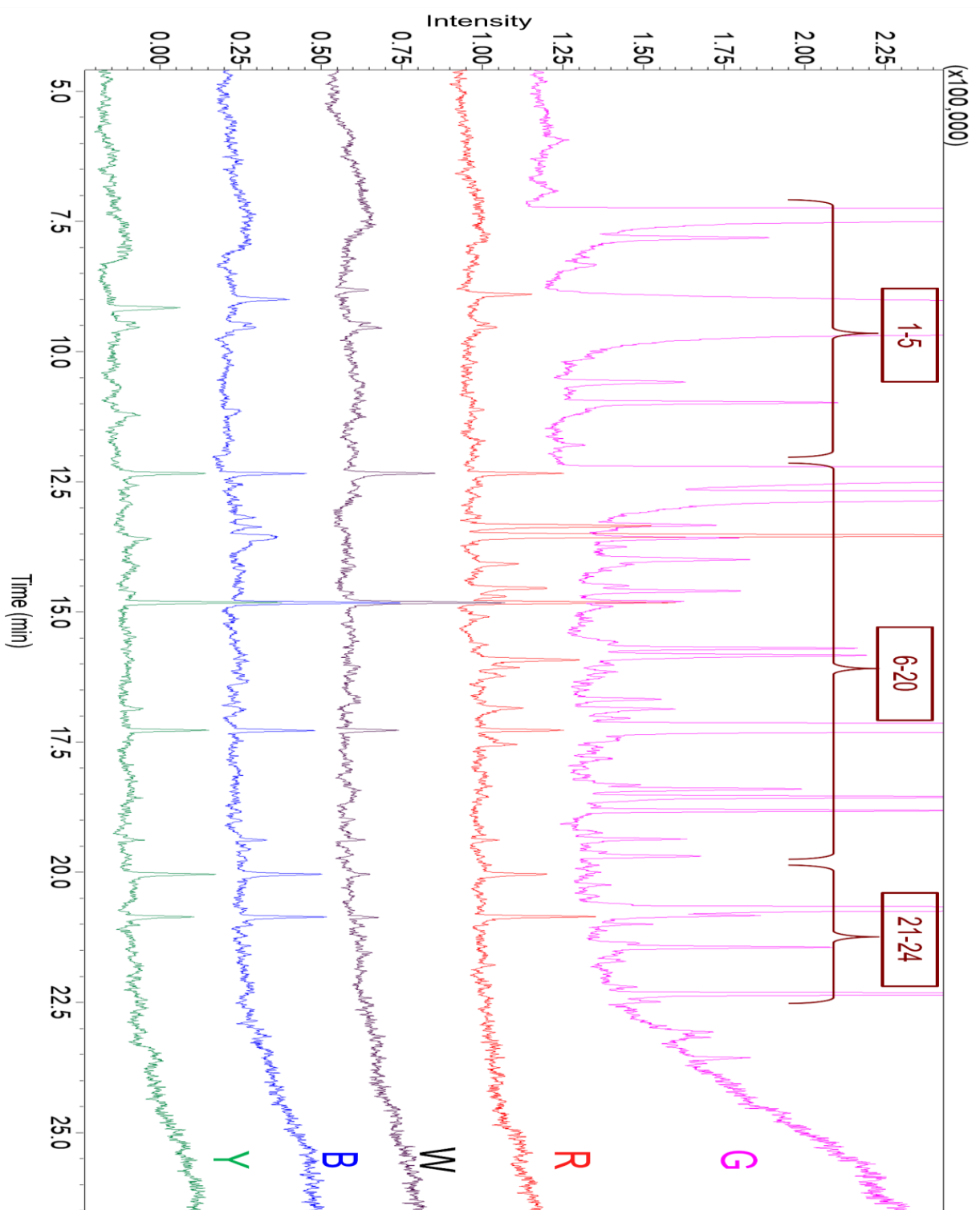


Figure S5. Chromatograms for HS/SPME injection of Waxy Dent (G), Red (R), White (W), Blue (B), and Yellow (Y) mash samples. Compound ID ranges are indicated above their respective retention time ranges.

Table S8. Compound ID's for HS/SPME injection of Red (R) mash

ID	tR(min)	Name
1	9.462	Hexanal
2	11.119	Methoxy-phenyl-oxime
3	12.786	2-Pentyl-furan
4	13.345	[[2-Ethylhexyl)oxy)methyl]-oxirane
5	13.534	Ethyl 2,2-diethoxypropionate
6	14.075	1,7-Octanediol, 3,7-dimethyl-
7	14.548	Ethyl linalool
8	14.706	7-Oxo-1,3,5-cycloheptatriene-1-carbonitrile
9	15.090	4,5-Dihydro-5,5-dimethyl-4-isopropylidene-1H-pyrazole
10	15.634	Pentafluoropropionic acid tridecyl ester
11	15.922	1-Pentadecyne
12	16.068	Diglycolic acid ethyl isobutyl ester
13	16.236	Carbonic acid nonyl vinyl ester
14	16.846	Dipropyl oxydiacetate
15	17.543	Myrtanyl 2-methylbutyrate
16	19.380	Phenylpyruvic acid oxime, 2TMS derivative
17	20.035	2,4-Di- <i>tert</i> -butylphenol acetate
18	20.853	4-Amino-N-(2-tetrahydrofurfuryl)-furazan-3-carboxamide

Table S9. Compound ID's for HS/SPME injection of White (W) mash

ID	tR(min)	Name
1	9.449	Hexanal
2	12.777	3-(2-Methylpropyl)-cyclohexene
3	20.039	2,4-Di- <i>tert</i> -butylphenol acetate

Table S10. Compound ID's for HS/SPME injection of Yellow (Y) mash

ID	tR(min)	Name
1	9.437	Hexanal
2	13.595	Ethyl 2,2-diethoxypropionate
3	16.854	Dipropyl oxydiacetate
4	20.040	2,4-Di- <i>tert</i> -butylphenol acetate

Table S11. Compound ID's for HS/SPME injection of Blue (B) mash

ID	tR(min)	Name
1	9.465	Hexanal
2	12.540	4-Ethyl-1-octyn-3-ol
3	12.564	1-Nonen-3-ol
4	13.184	1-Aminobenzotriazole
5	13.370	[[2-Ethylhexyl]oxy]methyl]-oxirane
6	13.550	Ethyl 2,2-diethoxypropionate
7	13.579	7-Isopropyl-2,3-diazabicyclo[2.2.1]hept-2-ene
8	20.037	2,4-Di- <i>tert</i> -butylphenol acetate

Table S12. Compound ID's for HS/SPME injection of Waxy Dent (G) mash

ID	tR(min)	Name
1	7.393	1-Butanol
2	8.330	1-Pentanol
3	9.589	Hexanoic acid
4	10.585	1-Hexanol
5	10.980	Methoxy-phenyl-oxime
6	12.393	1-Heptanol
7	12.763	Butanoic acid butyl ester
8	13.749	Butanoic acid 3-methylbutyl ester
9	13.996	Octyl-cyclopropane
10	14.497	4-Methylcyclohexanol acetate
11	14.597	Acetic acid heptyl ester
12	15.700	Benzoic acid 1-methoxy-1H-tetrazol-5-ylmethyl ester
13	15.833	Hexanoic acid hexyl ester
14	16.678	5,6-Decanediol
15	16.868	1,3- <i>bis</i> (1,1-Dimethylethyl)-benzene
16	17.257	Butanoic acid heptyl ester
17	18.402	5-Hexyldihydro-2(3H)-furanone
18	18.555	Octanoic acid hexyl ester
19	18.814	2,4,7,9-Tetramethyl-5-decyn-4,7-diol
20	19.244	1-Benzyloxy-3-methyl-2-butanol
21	20.998	2,6-Dihydroxybenzoic acid, 3TMS derivative
22	21.364	Unknown-1
23	22.335	Heptadecanoic acid butyl ester
24	22.490	7-Methyl-8(<i>Z</i>),10(<i>Z</i>)-hexadecadien-1-ol acetate

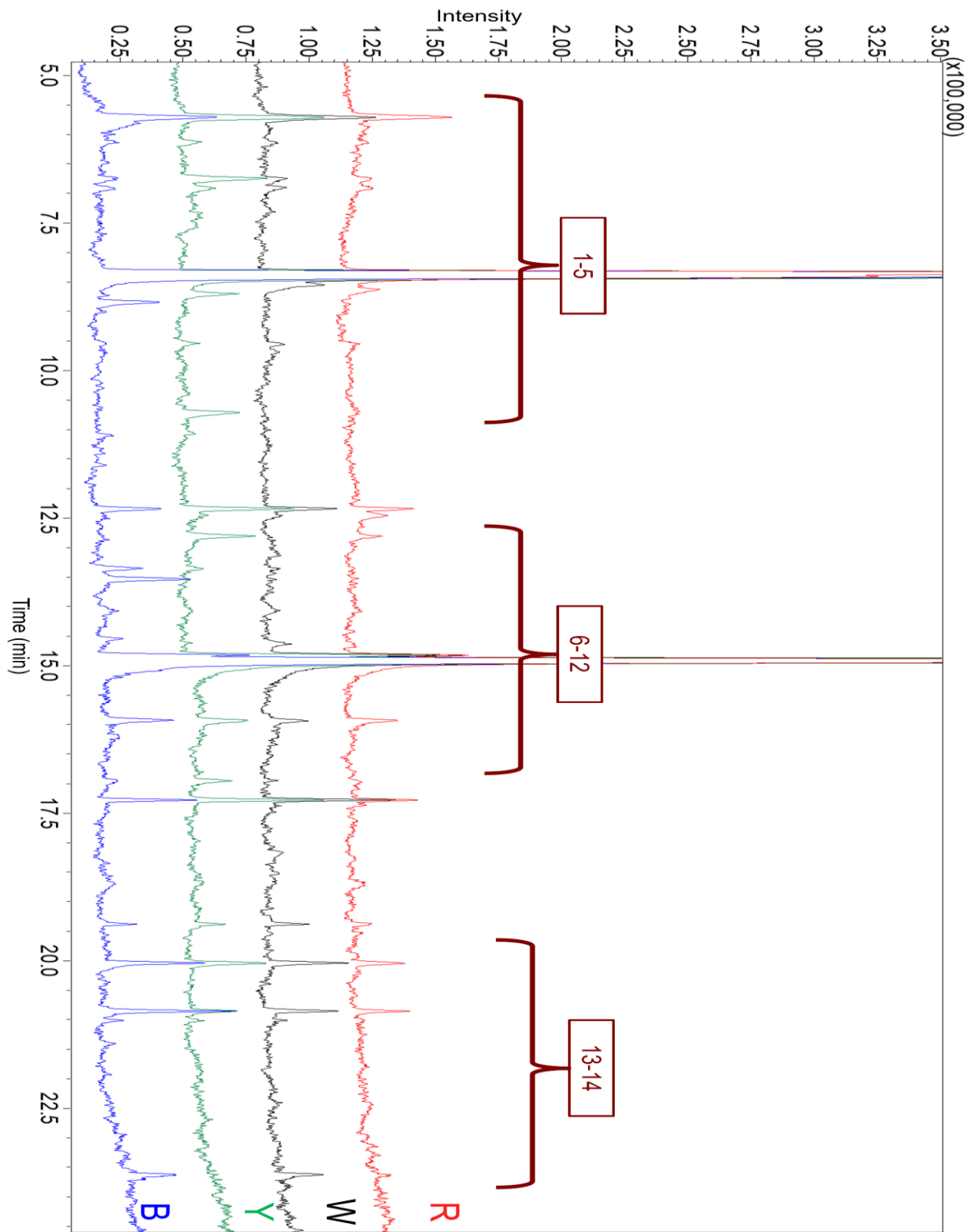


Figure S6. Chromatograms for HS/SPME injection of Red (R), White (W), Yellow (Y), and Blue (B) beer samples. Compound ID ranges are indicated above their respective retention time ranges.

Table S13. Compound ID's for HS/SPME injection of Red (R) beer

ID	tR (min)	Name
1	5.711	Boron trifluoride
2	6.747	Acetic acid pentyl ester
3	8.347	Dihydro-3,5-dimethyl-2(3H)-furanone
4	8.405	Succinic anhydride
5	12.458	α -Hydroxy-benzeneacetonitrile
6	12.807	Nonanoic acid ethyl ester
7	14.913	Benzyl isopentyl ether
8	15.933	Undecanoic acid ethyl ester
9	18.668	Methyl 2,6-dimethyltridecanoate
10	20.045	2- <i>tert</i> -Butyl-4-(1,1,3,3-tetramethylbutyl)phenol

Table S14. Compound ID's for HS/SPME injection of White (W) beer

ID	tR (min)	Name
1	5.713	Boron trifluoride
2	6.748	Acetic acid pentyl ester
3	6.900	Methyl valerate
4	8.349	Dihydro-3,5-dimethyl-2(3H)-furanone
5	8.407	Acetamide, N-2-propenyl-
6	8.551	Propane, 1-chloro-2-nitro-
7	14.636	<i>trans</i> -2-Undecen-1-ol
8	14.910	Benzyl isopentyl ether
9	15.939	Undecanoic acid ethyl ester
10	20.039	2- <i>tert</i> -Butyl-4-(1,1,3,3-tetramethylbutyl)phenol
11	21.011	3,4-Dihydroxymandelic acid, 4TMS derivative
12	23.626	Methyl 2,4-dimethylhenicosanoate

Table S15. Compound ID's for HS/SPME injection of Yellow (Y) beer

ID	tR (min)	Name
1	5.710	Boron trifluoride
2	6.126	Methylene chloride
3	6.744	Acetic acid pentyl ester
4	6.913	2-Methyl-4-propyl-oxetane
5	8.350	1-Hepten-3-one
6	10.713	2-Ethyl-2-methyl-1,3-propanediol
7	12.804	Nonanoic acid ethyl ester
8	13.358	Chloroacetic acid 2-ethylhexyl ester
9	14.911	Benzyl isopentyl ether

ID	tR (min)	Name
10	15.927	Undecanoic acid ethyl ester
11	16.954	2-Phenylethyl bromoacetate
12	20.041	2- <i>tert</i> -Butyl-4-(1,1,3,3-tetramethylbutyl)phenol

Table S16. Compound ID's for HS/SPME injection of Blue (B) beer

ID	tR (min)	Name
1	5.701	Boron trifluoride
2	6.739	Acetic acid pentyl ester
3	8.349	Dihydro-3,5-dimethyl-2(3H)-furanone
4	8.404	N-2-Propenyl-acetamide
5	11.106	Methoxy-phenyl-oxime_
6	13.351	6-Methyl-3(<i>E</i>)-undecene
7	13.535	Ethyl 2,2-diethoxypropionate
8	14.076	$\alpha,\alpha,4$ -Trimethyl-cyclohexanemethanol
9	14.542	Ethyllinalool
10	14.910	(Phenylmethyl)-hydrazine
11	15.926	8-Nonenoic acid ethyl ester
12	16.945	2-Phenylethyl bromoacetate
13	20.037	2- <i>tert</i> -Butyl-4-(1,1,3,3-tetramethylbutyl)phenol
14	23.635	Methyl 2,4-dimethylhenicosanoate